**Title**

# Fatigue Behavior in Medical Ultra High Molecular Weight Polyethylene (UHMWPE) for Total Joint Replacements (TJRs)



**ISBN**
9798189270581

**Author**
Smith, Bethany B

**Publication Date**
2026-05-01

Peer reviewed|Thesis/dissertation

# Fatigue Behavior in Medical Ultra High Molecular Weight Polyethylene (UHMWPE) for Total Joint Replacements (TJRs)

By

Bethany B. Smith

A dissertation submitted in partial satisfaction of the

requirements for the degree of

Doctor of Philosophy

in

Materials Science and Engineering

in the

Graduate Division

of the

University of California, Berkeley

Committee in charge:

Professor Robert O. Ritchie, Co-Chair
Professor Lisa A. Pruit, Co-Chair
Professor Phil Messersmith

Spring 2026

# Abstract

Fatigue Behavior in Medical Ultra High Molecular Weight Polyethylene for Total Joint Replacements

By

Bethany B. Smith

Doctor of Philosophy in Materials Science and Engineering

University of California, Berkeley

Professors Robert O. Ritchie and Lisa A. Pruitt, Co-Chairs

Total joint replacements (TJRs) are commonplace in the U.S., with over one million primary (i.e. first-time) knee and hip implant surgeries performed per year. The prevalence of primary total knee and total hip replacements is expected to nearly double by 2030, and of those implants, approximately 12% will require revision. The ultimate failure mode causing revision depends on many factors, but breakdown of the plastic component due to damage accumulation from mechanical fatigue is a leading concern. Fatigue failure is especially concerning in knees where cyclic contact stresses are elevated owing to concentrated loading across the condyles during normal articulation.

Ultrahigh-molecular-weight-polyethylene (UHMWPE) is the legacy material for the plastic components of TJRs, having been used since the 1960's and developed continuously since to meet market demands. UHMWPE is a semicrystalline polymer with molecular weights between 2-6 million g/mol, resulting in high chain entanglement and concordant high energetic toughness and abrasion resistance. Modern formulations of ultra-high are typically crosslinked to improve wear resistance, reducing ductility as a tradeoff. They may also have added antioxidants to regain some of the ductility lost from crosslinking, thus improving fatigue crack propagation (FCP) resistance at the cost of overall strength. Understanding the chemical and structural properties of UHMWPE that govern the balancing act between ideal fatigue, wear, and oxidation resistance results in a rich research design space, that, while parts of it have been thoroughly examined, other parts have yet to be documented.

While wear and oxidation resistance are major design considerations for UHMWPE, this dissertation focuses on the challenge of fatigue for this orthopedic polymer. Specifically, the two main points of this dissertation are to provide a literature review for fatigue in polymers in general and to add to UHMWPE literature by providing an initial study on the effect of the a/W ratio on cycles to failure and, more importantly, to provide the first record of fatigue crack threshold information across a wide variety of medical formulations of UHMWPE.

Chapter 1 serves as an introduction to UHMWPE for TJRs in general and why the studies included are relevant. Chapter 2 is a literature review about fatigue in polymers, providing information on the two primary fatigue design philosophies (total life vs. defect tolerant) and the effects of various factors on fatigue performance. Chapter 3 is an introductory exploration into the effect of notch root radius and a/W ratio on fatigue performance in two formulations of UHMWPE using a total life approach. Chapter 4 is a study using the defect tolerant (i.e. fracture mechanics) approach to understand both Paris regime and threshold behavior across a wide

variety of medical formulations of UHMWPE. Finally, Chapter 5 provides concluding remarks and future directions for UHMWPE fatigue research.

# Acknowledgements

It has been an incredibly long journey to earn this PhD. I'd like to thank my advisors, Lisa Pruitt and Rob Ritchie, for not giving up on me. To be honest it'd be understandable if they did considering how long things have taken. But I did it! Better late than never. I'd also like to thank all my friends and family that supported me along the way, especially my cats and Pete. To all the part time jobs I had to take, to my first advisor for firing me without a real cause,  and to all the people who said I couldn't do it – here's to you.

Table of Contents

# List of Figures

# List of Tables

# Chapter 1 – Introduction

Osteoarthritis affects more than 32.5 million people in the US and many times that number globally (“Osteoarthritis (OA) | Arthritis | CDC” 2020). Treatment options vary with disease severity and pain, and include exercise programs, targeted physical therapy, weight loss, medications, intra-articular injections, and, when conservative measures fail, total joint replacement (TJR) (“5 Ways to Manage Arthritis | CDC” 2023). In older adults, roughly 10% of men and 13% of women have symptomatic knee osteoarthritis, and about 20% have hip osteoarthritis (Zhang and Jordan 2010; Fan et al. 2023). These prevalence rates are expected to rise, increasing demand for TJRs and extending into younger age groups (S. Kurtz et al. 2007). Because this disease is so widespread and new populations are being affected, it is of utmost importance to design better TJRs. One way to do so is to better understand the materials used in orthopedic bearing systems so that TJRs can last longer, avoiding the revision surgeries that occur in about 10% of knee replacements and 7% of hip replacements at the 15 and 10 year marks respectively (Nugent et al. 2021; “Total Knee Replacement - OrthoInfo - AAOS” 2024).

Ultra-high-molecular-weight-polyethylene (UHMWPE) has been the material of choice for the bearing surface of total joint replacements (TJRs) since the early 1960’s (Charnley, 1973). The choice of UHMWPE arises from an array of unique bio-tribo-mechanical attributes including but not limited to abrasion and wear resistance, chemical inertness, energetic toughness, low friction, and biocompatibility (Kurtz, 2009). Despite its excellent bio-tribo-mechanical performance *in-vivo*, UHMWPE in total knee arthroplasty is subjected to high-amplitude cyclic contact stresses and must endure loading for 20-30 million cycles (Sobieraj & Rimnac, 2009). Such extensive biomechanical demands can culminate in the generation of sub-micron sized wear debris, leading to osteolysis, implant loosening, and eventually, failure of the TJR. In addition to the production of wear debris, catastrophic failure of the implant due to fast fracture from fatigue damage accumulation is also a potential issue (Ansari, Gludovatz, *et al*., 2016). In order to mitigate these potential failure modes, there is an ongoing effort to develop formulations of UHMWPE that resist the troika of challenges faced in the body – wear, fatigue, and oxidation (Ansari, Ries, *et al*., 2016; Atwood *et al*., 2011). Though no one specific formulation is ideal for every patient or failure modality, modern implants are typically made of moderately cross-linked UHMWPE which has been remelted with vitamin E additives, to protect it from oxidation while moderately balancing fatigue and wear properties (Bistolfi *et al*., 2021; Bracco & Oral, 2011). Understanding the interplay between these processing techniques, corresponding microstructures, and concomitant mechanical properties is an ongoing endeavor, even though the existing body of literature about UHMWPE for TJRs is quite extensive (Ansari, Gludovatz, *et al*., 2016; Ansari, Ries, *et al*., 2016; Baker *et al*., 2000, 2003; Connelly *et al*., 1984; Furmanski & Pruitt, 2007; Gencur *et al*., 2006; Patten *et al*., 2011; Pruitt, 2005; Pruitt *et al*., 2022; Simis *et al*., 2006; Sirimamilla *et al*., 2013a; Sirimamilla & Rimnac, 2019).

Though literature gaps exist for understanding the wear and oxidation resistance of UHMWPE as well, this dissertation focuses on fatigue behavior since it is such a major component in catastrophic TJR failure (Ansari, Gludovatz, *et al*., 2016) and because there were obvious literature gaps to fill. However, because fatigue is a complicated subject requiring much background knowledge to understand and interpret major results such as $\Delta K_{Threshold}$, Chapter 2 provides an extensive literature review of fatigue in polymers. Topics covered include the two primary design philosophies for fatigue life (total life and the defect-tolerant approaches), the basics of fracture mechanics, mechanisms that enhance fatigue performance, as well as various structural and environmental factors that affect fatigue behavior of polymers. Chapters 3 and 4 then fill in two of the previously mentioned literature gaps in understanding the fatigue behavior in UHMWPE: crack initiation and threshold behavior. Chapter 3 is an initial investigation into fatigue crack initiation in two medically relevant formulations, focusing on the effect of CT sample and notch geometries in UHMWPE. Though these findings are preliminary, the results remain useful in understanding the fundamental crack initiation behavior of an important orthopedic polymer. This is especially relevant considering paucity of crack initiation studies when compared to fatigue crack propagation studies for UHMWPE (Ansari, Ries, and Pruitt 2016; L. Pruitt, Wat, and Malito 2022; Furmanski and Pruitt 2007; Patten et al. 2011a; Ansari et al. 2016; Furmanski and Pruitt 2018; Baker, Hastings, and Pruitt 1999; 2000; Baker, Bellare, and Pruitt 2003; Bradford et al. 2004; L. A. Pruitt et al. 2005; Ries and Pruitt 2005; Simis et al. 2006).

However, the most important findings of this dissertation are found in Chapter 4. Until this dissertation and the journal article resulting from it were published, there were no known publications of fatigue crack threshold behavior for UHMWPE, which is surprising considering its status as the legacy material for TJRs. Though the Paris fatigue regime was characterized as well, the opus of this study was determining fatigue threshold information for six (6) medically relevant formulations of UHMWPE. The fatigue properties were then related to their structural variables (crystallinity, lamellar size, degree of crosslinking), chemical formulations (molecular weight and antioxidants), and quasi-static monotonic mechanical properties (yielding, tensile strength, fracture strain, modulus and fracture toughness). From this all-encompassing approach, we gained a thorough understanding of the relationships between microstructural/chemical properties and fatigue properties in UHMWPE that incorporates the materials science structure-property-processing framework. Finally, Chapter 5 wraps up the dissertation by providing concluding remarks and future directions for research in fatigue of UHMWPE. The author hopes that this dissertation will serve as a comprehensive resource for understanding modern findings in fatigue of clinically relevant formulations UHMWPE as well as broadly guiding the understanding of fatigue behavior of polymers for load-bearing applications.

# Chapter 2 – Fatigue of Polymers

*This chapter has been published in the 2nd Edition of the Comprehensive Structural Integrity book (Pruitt, Roy, and Smith 2023)*

## 2.1 Introduction

Fatigue of polymers is of critical concern to the engineering community as plastics have been increasingly incorporated into load-bearing applications over the last few decades. Polymers offer a variety of unique properties including low density, chemical inertness, lubricity, good specific strength and modulus, as well as cost effectiveness. These properties have made plastic materials ideal candidates for applications in the automotive, aerospace, sporting goods, and medical industries. When designing polymeric components for structural applications involving cyclic loading conditions, understanding fatigue resistance is of paramount importance. As with other engineering materials, failure often ensues in the polymer as a result of accumulated damage, or growth of a defect to a critical dimension. The fatigue performance of polymers is extremely sensitive to the molecular structure of the polymer. Molecular variables include molecular weight, molecular weight distribution, crystallinity, chain entanglement density, crosslink density, and the presence of fillers or reinforcements. Most polymers are viscoelastic and hence are sensitive to frequency, waveform, along with service temperatures. In addition to molecular factors, the fatigue life of a polymeric component is controlled by a number of mechanical factors including the stress or strain amplitude of the loading cycle, the mean and peak stress of the cycle, and the presence of stress concentrations or initial defects in the component. All of these factors are of considerable interest and practicality for the safe design of structural polymeric components that are subjected to fatigue loading.

Characterization of fatigue behavior of an engineering polymer generally entails the use of one of two distinct design philosophies. The first of these, commonly used in applications where the majority of the fatigue life is spent in the nucleation of a flaw, is termed as the total life approach. This design methodology assumes that the component is initially defect-free and fatigue characterization is typically performed with unnotched specimens that are free of substantial stress concentrations. This methodology is based on the notion that fatigue failure is a consequence of crack nucleation and subsequent growth to a critical size. The total life philosophy is distinct from the defect-tolerant approach, in which the fatigue life of a component is based on the number of loading cycles needed to propagate a crack of an initial size to a critical dimension. The defect-tolerant philosophy is commonly employed in safety-critical applications such as medical devices. In light of this, it is important to note that the literature generally makes a clear distinction between crack initiation and propagation studies, which then go on to emulate the total-life and defect-tolerant philosophies, respectively. Over the last few decades, researchers have provided a number of detailed reviews that speak to the various factors contributing to the fatigue performance of engineering polymers (Andrews 1969; Beardmore and Rabinowitz 1975; Sauer and Richardson 1980; Sauer and Hara 1990; Hertzberg et al. 1979; O'Connell and Mckenna 2002; Naebe et al. 2016; Awaja et al. 2017; Hertzberg and Manson 1980, 1986; Kausch and Williams 1986; Ferry 1961). These reviews encompass the fatigue behavior in polymers based on both total-life and fracture-mechanics approaches.

This article first explores fatigue life estimation approaches viz. total-life philosophy which includes both stress and strain-based loadings. The defect-tolerant philosophy predicated on fracture-mechanics follows with discussion of crack shielding and toughening mechanisms in polymeric materials. The subsequent section then laboriously compiles the molecular and mechanical factors that influence the fatigue characteristics of polymers.

The aim of this chapter is to provide a general overview of the fatigue behavior of engineering polymers. To accomplish this, a number of the original pioneering works on fatigue of polymers are cited as well as the recent advances in the field are included. The chapter also qualitatively and quantitatively presents the overall fatigue landscape vis-à-vis polymers.

## 2.2 Total-Life Philosophy

### 2.2.1 Stress-Based Loading

The total-life philosophy is founded on the premise that the component is initially defect-free, and that the life of a polymeric component is based on the initiation of a flaw and subsequent growth to a critical crack size. Damage is accumulated until a flaw nucleates. Failure ensues (i.e. the sample rips in half) as the specimen accommodates a critical level of damage. The preponderance of polymer fatigue characterization based on this design philosophy is performed under stress-controlled conditions. In these tests, unnotched specimens are generally subjected to constant-amplitude load cycles until failure occurs.

In fatigue testing, the applied stress, $\boldsymbol{\sigma}_a$, is typically described by the stress amplitude of the loading cycle and is defined as:

$$\sigma_a = \frac{\sigma_{max} - \sigma_{min}}{2} \qquad \text{Eq. [1]}$$

where $\boldsymbol{\sigma}_{max}$ is the maximum stress and $\boldsymbol{\sigma}_{min}$ is the minimum stress of the loading cycle. Once many samples are tested, an S-N plot is generated by plotting the stress amplitude (S) against the number of cycles to failure (N) on a linear-log scale, each broken sample as its own data point. Starting at high stress amplitudes, samples are broken at increasingly smaller values of stress amplitude until an endurance limit is reached ($\boldsymbol{\sigma}_e$). An endurance limit is defined as the stress level that results in more than 10 million cycles without failure. The assumption is that if the device is exposed to stress amplitudes below $\boldsymbol{\sigma}_e$, then the device is safe from fatigue failure (it is noteworthy, that not all polymers have an endurance limit). S–N curves enable life to be predicted based on the stress amplitude or range of stress amplitudes that a component is expected to encounter.

Figure 1 shows the S–N behavior of several commodity plastics. Polymers such as polyethylene (PE), polypropylene oxide (PPO), polystyrene (PS), polytetrafluoroethylene (PTFE), polypropylene (PP), polymethyl methacrylate (PMMA), and epoxy (EP) clearly exhibit an endurance limit below which failure does not occur in less than $10^7$ cycles. On the other hand, nylon and polyethylene terephthalate (PET) do not exhibit endurance limits (the slopes of their S-N curves do not approach zero nor do the curves become asymptotes to any line parallel to the horizontal axis). The specifics of why some polymers exhibit an endurance limit while others do not is a current area of research and has garnered significant attention in the polymer community. However, it is generally accepted that the measured endurance limit in polymeric glasses is a result of the polymer's previous stress and temperature states (Pastuhov et al. 2020). Called "progressive aging", the evolution of a polymer's properties throughout its characterization and service life affects many important mechanical attributes. It is therefore of paramount importance to understand the processing history of the polymer and the conditions under which the mechanical testing is performed, so that any design decisions based on those mechanical properties are sound.

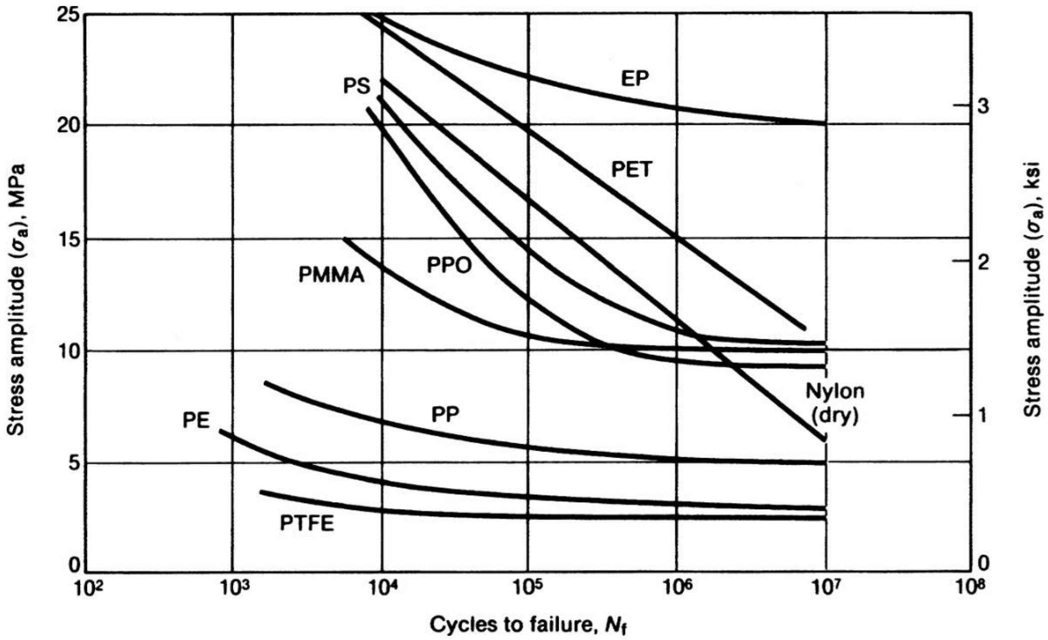


**Figure 1** Stress amplitude vs. cycles to failure (S–N behavior) of several commodity plastics. (Hertzberg and Manson 1980)

The total life fatigue performance of polymers is sensitive to many experimental factors including test frequency, temperature, and mean stress. In addition, fatigue performance is also heavily influenced by molecular factors such as chemistry, molecular weight, crystallinity, and degree of crosslinking. These factors will be explored in greater detail in later sections. While there are ASTM and ISO standards (E647 and 12110-1:2013, respectively) which stipulate the specifics of the test conditions for ensuring standardization, it is essential that the fatigue test conditions closely mimic the service conditions of the polymeric component and customization is often vital for polymeric testing. In sum, the S–N approach is widely accepted in the engineering plastics community for design applications where stress concentrations are expected to be minimal or where the fatigue life of the component is likely to be dominated by the nucleation of a crack, a.k.a. crack initiation.

### 2.2.2 Strain-Based Loading

Strain-based tests are often utilized to characterize polymers when the structural component is likely to experience fluctuations in displacement or strain and are often utilized for components with accumulated strain or blunt notches (Hertzberg and Manson 1980). Most strain-based fatigue tests are performed using fully reversed loading conditions. In general, this is accompanied by a cyclic softening phenomenon in plastics (Ferry 1961; Beardmore and Rabinowitz 1975; Landel and Nielsen 1993; Krzypow and Rimnac 2000). Under cyclic strain conditions, the fatigue response is best characterized by the cyclic stress–strain curve. Figure 2 shows a comparison of the cyclic and monotonic (tension) stress–strain curves for nylon, polycarbonate (PC), polypropylene, and acrylonitrile butadiene styrene (ABS). An interesting attribute of these plots is that all of these polymers cyclically soften with lower yield points than their quasi-static values. Polymers generally soften under cyclic loading conditions, rather than cyclically harden as is observed in many structural metals.

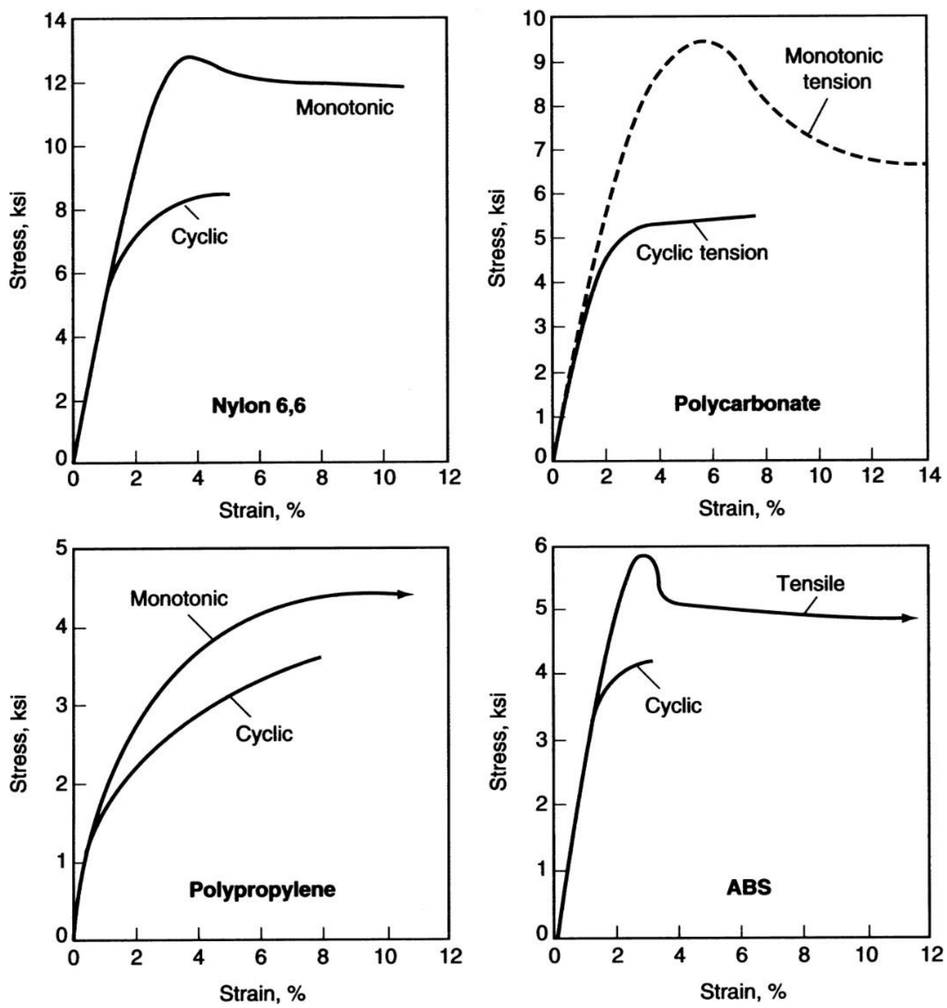


**Figure 2** Comparison of the cyclic and monotonic (tension) stress–strain curves for nylon, polycarbonate, polypropylene, and acrylonitrile butadiene styrene (ABS). (Hertzberg and Manson 1980)

Cyclic strain data can also be represented in a manner that is analogous to the S–N characterization. The total strain amplitude can be divided into the elastic and plastic strain amplitude components. In these tests, the strain amplitude of the fatigue cycle is plotted against the number of cycles or load reversals to failure. This provides an empirical relationship between the strain amplitude of the fatigue cycle and the number of cycles to specimen failure (Hertzberg and Manson 1986):

$$\epsilon_a = \frac{\sigma_f'}{E}\left(2N_f\right)^b + \epsilon_f'\left(2N_f\right)^c \qquad \text{Eq. [2]}$$

Equation [2] is commonly known as the Coffin-Manson equation. Here $\boldsymbol{\varepsilon}_a$ is the strain amplitude, $\boldsymbol{\sigma}'_f$ is the strength coefficient, $\boldsymbol{\varepsilon}'_f$ is the ductility coefficient, $\boldsymbol{2N_f}$ is the number of load reversals to failure, and b and c are material constants. The first term on the right-hand side of Equation [2] represents the elastic component of the strain amplitude, while the second term signifies the plastic component of the strain amplitude. Tests dominated by small amounts of cyclic plastic strain are designated high-cycle fatigue while those with high plastic strains are termed low-cycle fatigue. The former is characterized by a large number of cycles to failure and the latter is identified by the relatively small number of cycles to failure. In between these two extremes lies the transition life $2N_t$, which marks the distinction between high-cycle and low-cycle fatigue and is ascertained by equating the elastic and plastic components of the strain amplitude and thereafter, solving for the number of cycles to fatigue failure $2N_t$:

$$\frac{\sigma_f'}{E}(2N_t)^b = \epsilon_f'(2N_t)^c \qquad \text{Eq. [3]}$$

Solving for $2N_t$, we get:

$$2N_t = \left(\frac{\epsilon_f' E}{\sigma_f'}\right)^{\left(\frac{1}{b}-c\right)} \qquad \text{Eq. [4]}$$

It is paramount to consider the attributes of the fatigue test since those guide the relative ranking of fatigue resistance amongst various polymers. For example, polymers with higher damping capacities may be less resistant to fatigue. This is due to thermal heating when tested under constant stress amplitude. Conversely, these same polymers may have enhanced fatigue resistance if tested under constant deflection conditions. Moreover, the relative placement of fatigue resistance in polymers is correlated strongly with whether the tests are performed under adiabatic or isothermal conditions (Hertzberg and Manson 1980). These factors are important considerations to make when designing fatigue tests for the evaluation of polymeric components.

## 2.3 Defect-Tolerant Philosophy

### 2.3.1 Fracture Mechanics Concepts

The defect-tolerant philosophy is based on the implicit assumption that structural components are intrinsically flawed and that the fatigue life is based on the propagation of an initial flaw to a crack of critical size (Ritchie and Liu 2021). Linear elastic fracture mechanics (LEFM) is used to analyze the propagation of fatigue cracks in advanced engineering plastics that are capable of sustaining a large amount of subcritical crack growth prior to fracture. The defect-tolerant approach is used in safety-critical applications such as aerospace, pressure vessels, and medical applications (Kurtz 2009). Fatigue crack propagation (FCP) resistance in polymers is influenced by near-tip micro-mechanisms, mean stress, frequency, and environment (Hertzberg and Manson 1983). Such factors complicate fatigue characterization as cracks may advance at different rates depending on their propensity. Understanding the effects of molecular and mechanical factors is of critical importance for the safe design of structural polymeric components subjected to repetitive loading. These influences are explored after a brief review of linear elastic fracture mechanics as it is utilized in crack propagation studies.

The stress intensity factor, K, derived from linear elastic fracture mechanics is the parameter used to describe the magnitude of the stresses, strains, and displacements ahead of the crack tip. The linear elastic solution for the normal stress in the opening mode of loading is written as a function of distance, r, and angle, $\boldsymbol{\theta}$, away from the crack tip (Sih 1973):

$$\sigma_{yy} = \frac{K_I}{\sqrt{2\pi r}} cos\frac{\theta}{2} \left(1 + \sin\frac{\theta}{2} sin\frac{3\theta}{2}\right) \quad \text{Eq. [5]}$$

where $K_I$ is the mode I (opening mode) stress-intensity factor. The stress-intensity parameter incorporates the boundary conditions of the cracked body and is a function of loading, crack length, and geometry. The stress-intensity factor can be found for a wide range of specimen types and is used to scale the effect of the far-field load, crack length, and geometry of the flawed component.

LEFM provides a conservative design approach for predicting the life of a cracked structural component under cyclic loading conditions. Although the fracture micro-mechanisms vary for metals, polymers, and ceramics, the fatigue crack propagation behavior of these materials shares many similar attributes at the macroscopic scale. As with other engineering materials, there are three distinct regimes of crack propagation for polymers under constant amplitude cyclic loading conditions viz. zone A: near-threshold regime, characterized by slow crack growth and below which, crack propagation doesn't occur; zone B: intermediate crack growth regime a.k.a. Paris regime; and zone C: fast crack propagation regime, commonly referred to as the unstable crack growth regime which is dominated by $K_{max}$. These regimes are denoted in Figure 3 which shows typical crack growth rate (velocity) plotted against the cyclic stress intensity range (illustrated on a log–log scale). Ultimately, the curve reaches a stage where it becomes an asymptote, corresponding to $K_{max} \rightarrow K_c$, where $K_c$ is the fracture toughness of the material under study (Dowling 1993). The velocity of a moving fatigue crack subjected to a constant stress amplitude loading is determined from the change in crack length, *a*, as a function of the number of loading cycles, *N*. This velocity represents the fatigue crack growth per loading cycle, *da/dN*, and is found from experimentally generated curves where *a* is plotted as a function of *N*. Paris and co-workers suggested that the stress-intensity factor range, $K= K_{max} - K_{min}$ which itself captures the far-field stress, crack length, and geometry, should be the characteristic driving force parameter for fatigue crack propagation (Paris et al. 1961). This is known as the Paris Law, and it states that *da/dN* scales with $\Delta K$ through the following power-law relationship:

$$\frac{da}{dN} = C\Delta K^m \quad \text{Eq. [6]}$$

where C and m are material constants. The Paris equation is valid for intermediate $\Delta K$ levels spanning crack propagation rates from $10^{-6}$ to $10^{-4}$ mm/cycle, which is considered the universal range for the Paris regime (Suresh 1998). The Paris regime is most often used for life prediction, although the fatigue threshold is key for designing against the inception of crack growth where components are expected to have long service lifetimes or where intermittent inspections may be difficult, such as in the medical device industry.

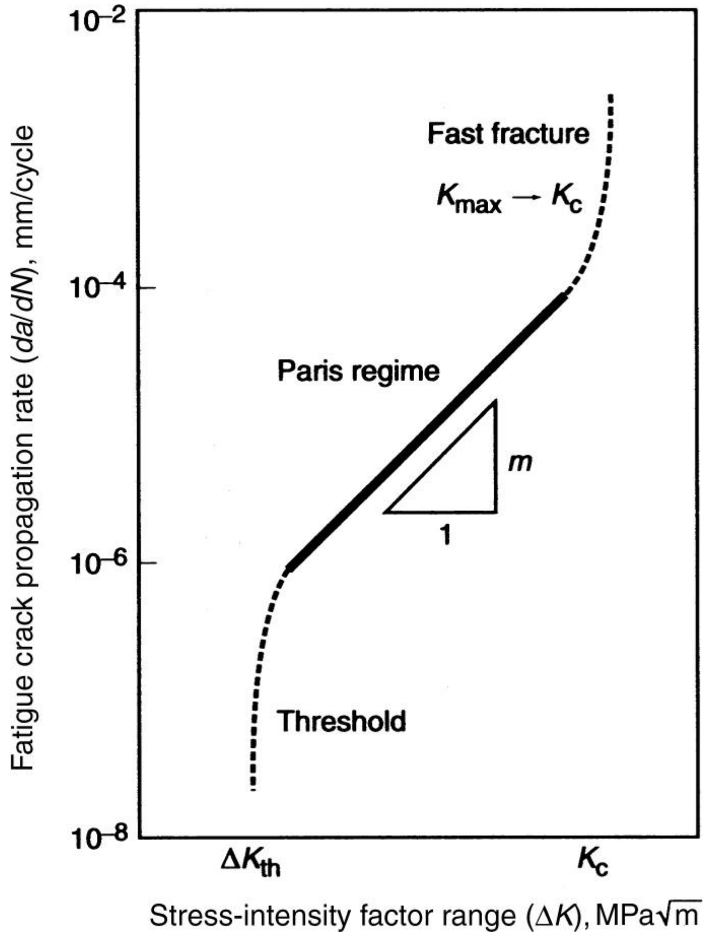


**Figure 3** Illustration of the sigmoidal curve that captures the crack growth rate as a function of stress-intensity range (illustrated on a log–log scale).

The Paris Law is commonly employed for fatigue-life prediction of polymer components that have known stress concentrations and for which small scale yielding conditions prevail. It is worth noting that not all polymers lend themselves to the use of linear elastic fracture mechanics, some ductile thermoplastics lend themselves better to assessment through elastic-plastic fracture theories or viscoelastic models (Hertzberg and Manson 1983). It is implied in the use of an LEFM defect-tolerant approach that the device or component contains an initial defect or crack size, $a_i$. This can be determined from non-destructive evaluation (NDE), and if no defect is found, an initial defect whose size is the limit of resolution of the NDE method is assumed to exist. Assuming that the fatigue loading is performed under constant stress amplitude conditions, that the geometric factor, $f(\boldsymbol{\alpha})$, does not change within the limits of integration, and that fracture occurs when the crack reaches a critical value, $a_c$, one can integrate the Paris equation to predict the total fatigue life of the component:

$$N_f = \frac{2}{(m-2)C\, f(\alpha)^m (\Delta\sigma)^m \pi^{\frac{m}{2}}} \left( \frac{1}{a_i^{\frac{m-2}{2}}} - \frac{1}{a_c^{\frac{m-2}{2}}} \right) \text{for } m \neq 2 \qquad \text{Eq. [7]}$$

### 2.3.2 Crack-Shielding Mechanisms in Polymers

Crack shielding occurs when the crack driving force near a fatigue crack tip, $\Delta K_{tip}$, is lower than the 'applied' crack driving force, $\Delta K_a$, and this phenomenon is also known as extrinsic toughening (Ritchie and Liu 2021). Extrinsic toughening mechanisms shield the crack tip from the full effect of the applied crack driving force and hence, lower the crack growth rate. While extrinsic toughening mechanisms work behind the crack tip, intrinsic toughening mechanisms take place ahead of the crack tip and occur in the form of dissipative processes, redirecting the additional energy from crack growth to some form of microstructural alteration such as crazing, fibrillation or blunting (Pippan and Hohenwarter 2017). There are several shielding/toughening mechanisms that may be activated in polymers or polymer blends, both intrinsic and extrinsic and these include: (1) crack deflection; (2) particle tearing; (3) bridging by fibers, ligaments, or second-phase particles; (4) massive shear banding; (5) plastic void growth; (6) multiple craze formation or microcracking; (7) zone shielding through phase transformations; or (8) contact shielding from surface asperity contact or plasticity induced closure (Lampman 2003). The extrinsic crack-tip shielding effect has been expressed (Ritchie 1988) as:

$$\Delta K_{tip} = \Delta K_{\boldsymbol{a}} - K_S \qquad \text{Eq. [8]}$$

where $K_S$ is the stress-intensity factor due to shielding. There are three general classes of shielding mechanisms that operate under cyclic loading conditions: crack deflection, zone shielding, and contact shielding. Crack deflection results in improvements in the fatigue crack propagation behavior over all ranges of $\Delta K$. Contact shielding mechanisms are more effective at low $\Delta K$ levels, while process-zone shielding mechanisms operate more effectively at high $\Delta K$ levels (Ritchie 2000).

The crack-tip shielding process that results in crack path deflection has been previously modelled (Suresh 1998). He derived the effective fatigue crack driving force and subsequent crack growth rates by analyzing a small segment of the crack with an out-of-plane deflection:

$$\Delta K_{tip} = \frac{b \cos^2\left(\frac{\theta}{2}\right) + c}{b + c} \Delta K_a \qquad \text{Eq. [9]}$$

and

$$\frac{da}{dN} = \frac{b \cos\theta + c}{b + c} \left(\frac{da}{dN}\right)_n \qquad \text{Eq. [10]}$$

where $\theta$ is the deflection angle, b is the deflected distance, c is the undeflected distance, and $(da/dN)_n$ is the propagation rate of a straight crack subjected to the same effective driving force.

The amount of shielding due to process-zone mechanisms depends on the size of the process zone and micro-mechanisms activated ahead of the crack tip. For polymers, these may include lamellar reorientation, phase transformations, crazing, or shear banding (Evans et al. 1986; Bucknall and Stevens 1978; Hertzberg 1996; Anderson 1995; Argon 1989; Plummer and Kausch 1996; Ansari 2015). The yielding in front of the crack due to far-field tensile loading results in the formation of a plastic or permanent deformation zone. For example, in a crazeable polymer, amorphous chains are reorganized into load-bearing fibrils ahead of the crack tip, that are aligned with principal tensile stress. For this micro-mechanism, a Dugdale or strip yield approximation

(Estevez and Van der Giessen 2005) is used to estimate the size of this plastic zone (Suresh 1998):

$$r_d = \frac{\pi}{8}\left(\frac{K_I}{\sigma_y}\right)^2 \qquad \text{Eq. [11]}$$

For an elastic, perfectly plastic material behavior, the plastic zone, $r_p$, can be estimated as (Suresh 1998):

$$r_p \approx \frac{\mathbf{1}}{\boldsymbol{\pi}}\left(\frac{K_I}{\sigma_y}\right)^2 \qquad \text{Eq. [12]}$$

In equations [11] and [12] above, $\boldsymbol{\sigma_y}$ depicts the craze stress or yield stress, respectively and $K_I$ is the mode I stress intensity factor. Qualitatively, it is easy to see that the size of the plastic zone increases with $\Delta K$. Therefore, process-zone shielding mechanisms are most effective at high $\Delta K$ levels.

Contact shielding involves the physical contact between mating crack surfaces due to the presence of asperities, second-phase particles, and/or fibers. Premature contact between the crack surfaces occurs during unloading at a stress-intensity level known as $K_{cl}$, which is often referred to as the closure stress intensity. The amount of shielding due to closure effects can be calculated from:

$$\Delta K_{tip} = K_{max} - K_{cl} \qquad \text{Eq. [13]}$$

where $K_{max}$ is the maximum stress intensity of the fatigue cycle (Ritchie 2002). Additionally, fiber bridging has been shown to be a viable shielding mechanism in short fiber composites (Lang et al. 1984).

### 2.3.3 Toughening Mechanisms in Polymers

Toughening mechanisms are often divided into two categories: those involving the process zone ahead of the crack tip and those which occur behind the crack tip as illustrated in Figure 4. Some polymeric structures such as rubber-toughened polymers can activate both mechanisms to obtain synergistic toughening (Pearson and Pruitt 1999). The process-zone mechanism of toughening is typically described using crack-tip energetics (Kinloch and Guild 1996; Clark et al. 1991; Kramer and Berger 1990; Azimi et al. 1996; Quaresimin et al. 2015).

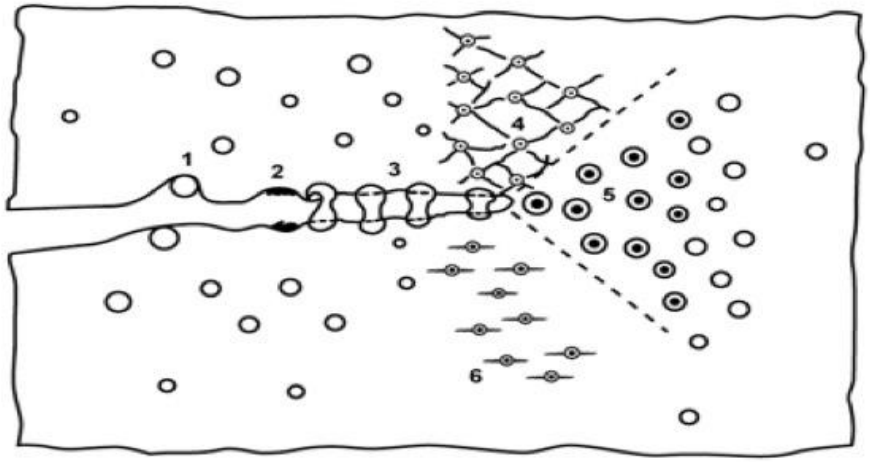


**Figure 4** Schematic showing a range of micro-mechanisms that may be activated in polymers or reinforced polymer systems. These include (1) crack deflection; (2) particle tearing; (3) bridging by fibers or second phase particles; (4) massive shear banding; (5) plastic void growth; and (6) multiple craze formation or microcracking (Pearson and Pruitt 1999).

The energy release rate, $G$, characterizes the release in potential energy with advancement of the crack front. The energy release rate is related to the stress-intensity parameter under linear elastic conditions (plane strain) and can be written as $G = K^2/E$, where $E$ is the elastic modulus and $K$ is the stress intensity factor (Suresh 1988). If one considers a polymeric material that generates a process zone of width equal to $2w$ at its crack tip, then as the crack advances through the material, it leaves a wake behind the crack tip. The change in toughness due to energy changes in the strip is given as (Anderson 1995):

$$\Delta G_c = 2\int_0^w \int_0^{\varepsilon_{ij}} \sigma_{ij} \varepsilon_{ij} dy \qquad \text{Eq. [14]}$$

where the second integral represents the strain energy density. The critical energy release rate for propagation is then equal to the work required to advance the crack from $a$ to $a+da$ (normalized by the new crack area, $da$ (for unit thickness)):

$$G_c = \Delta G_c + G_i = 2\int_0^w \int_0^{\varepsilon_{ij}} \sigma_{ij} \varepsilon_{ij} dy + 2y_e \qquad \text{Eq. [15]}$$

where $G_i$ is the intrinsic toughness and $\Delta G_c$ is the energy to generate new crack surfaces under elastic conditions. An analogous form can be developed for non-linear deformations by using the J-integral approach (Evans et al. 1986): $J_C = \Delta J_C + J_i$.

If the reinforcing particles are responsible for all of the energy dissipation, one can assume the strain energy does not depend on y (the normal direction to the crack plane). For $f$ particles per unit volume, one can write the toughness as (Anderson 1995):

$$G_c = 2wf \int_0^{\varepsilon_{ij}} \sigma_{ij} \boldsymbol{\varepsilon}_{ij} dy + 2y_e \quad \text{Eq. [16]}$$

Particle bridging provides another mechanism of toughening. Here, an advancing crack leaves second phase particles intact behind the crack tip as it advances through the polymeric material. It was shown that rubber particle bridging and tearing could lead to improvements in toughening (Ahmad et al. 1986). Many toughened polymer systems utilize second phase additions capable of non-linear deformation and in such instances non-linear elastic fracture mechanics may be utilized (Evans et al. 1986; Kinloch and Guild 1996).

Many of these toughening mechanisms are activated in rubber-toughened polymers through rubber particle bridging and cavitation as well as matrix plasticity resulting in the nucleation of multiple crazes and shear bands (discussed above). Numerous theories are postulated on the predominance, ordering and synergistic effect of these mechanisms (Argon 1989; Evans 1986; Kinloch and Guild 1996). In summary, extrinsic and intrinsic shielding and toughening mechanisms can be synergistically and efficiently utilized in order to improve fatigue crack propagation resistance in engineering polymers as demonstrated from the aforementioned sub-sections. Together, they shield the crack tip from the driving force trying to open the crack front as well as induce microstructural changes which prevent the crack from propagating further, both behind and in front of the crack tip.

## 2.4. Factors Affecting Fatigue Performance of Polymers

### 2.4.1 Molecular Variables

The fatigue behavior of polymers is strongly affected by their molecular structure. Polymers with the same backbone chemistry can still vary immensely in their structure owing to a broad range of molecular variables. These include molecular weight, crystallinity, chain entanglement density, degree of crosslinking, as well as the contributions of fillers or reinforcements (Sauer and Richardson 1980; Hertzberg and Manson 1980; Lang et al. 1984; Kinloch and Guild 1996; Clark et al. 1991; Ansari 2015; Kishi et al. 2021). As a general rule, polymers with higher molecular weights and crystallinity exhibit an increased resistance to fatigue damage.

Figure 5 shows a comparison of fatigue crack propagation behavior for several amorphous and semicrystalline polymers. From this figure it can be deduced that semi-crystalline polymers exhibit the greatest resistance to crack propagation.

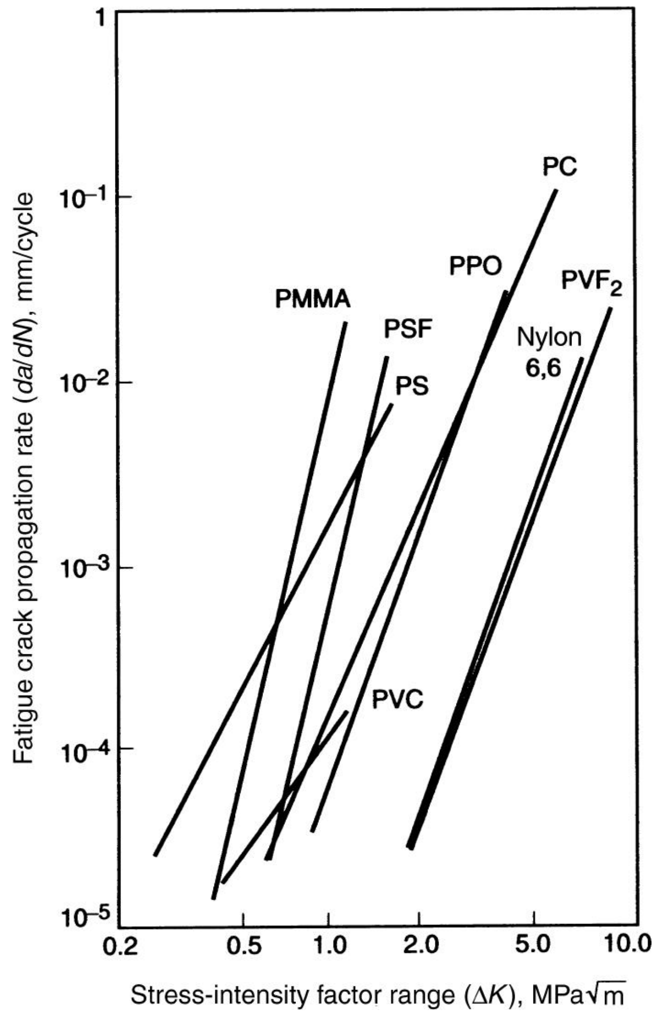


**Figure 5** Comparison of fatigue crack propagation behavior in the Paris regime for several amorphous and semi-crystalline polymers. Note the enhanced fatigue resistance of the semicrystalline polymers (Hertzberg and Manson 1980).

The fatigue characteristics of ultra-high molecular weight polyethylene (UHMWPE) across various formulations has been investigated in previous studies (Pruitt et al. 1992; Pruitt 1993; Baker et al. 2003, Atwood et al. 2011; Ansari 2015; Pruitt et al. 2013; Ansari et al. 2016). For UHMWPE resins of equivalent molecular weight, an increase in crystallinity results in a proportional increase in the crack inception stress-intensity values ($\Delta K_{inception}$). Similar trends are observed with molecular weight. Higher molecular weight formulations provide the greatest toughness and resilience to crack growth. However, resistance to fatigue crack growth can be diminished through crosslinking.

Figure 6 shows the effect of crosslinking on the fatigue crack propagation resistance of UHMWPE. It is pertinent to note here that increasing the amount of radiation dosage concomitantly increases the amount of crosslinking in UHMWPE. Crosslinking restricts flow of the amorphous chains and lamellar plasticity, resulting in a diminished resistance to crack growth (Baker et al. 2003; Atwood et al. 2011; Pruitt et al. 2013; Ansari et al. 2016).

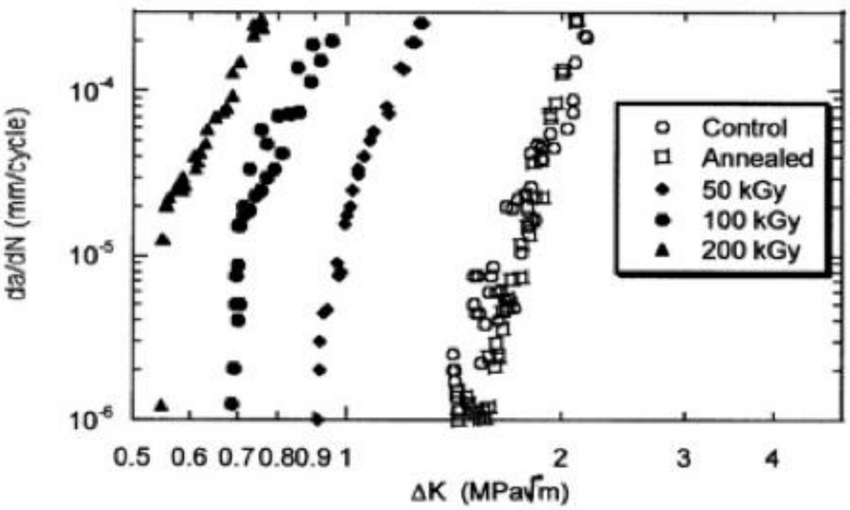


**Figure 6** Plot showing the effect of crosslink density on the fatigue crack propagation resistance of UHMWPE. The radiation dose is directly related to the amount of crosslinking present in the UHMWPE microstructure (Baker et al. 2003).

Many amorphous polymers are susceptible to craze nucleation in the presence of hydrostatic stress states (Sauer and Richardson 1980; Kramer and Berger 1990). Under cyclic tension, crazes can lead to subsequent crack growth and fatigue failure. Mechanistically, this occurs after a critical amount of damage has accumulated, advancing the crack advances through rupture of the leading fibrils in the craze zone (Hertzberg and Manson 1980; Argon 1989). This process often occurs through a void growth mechanism that can be exacerbated by temperature, chemical environment, or rupture of the highly stressed fibrils; crazes often advance in an intermittent manner and can results in discontinuous fatigue crack growth (Hertzberg and Manson 1980).

It has been shown that the craze stability depends on numerous factors, including the molecular weight and chain entanglement density of the polymer (Kramer and Berger 1990). The stability or strength of the craze is generally improved by increasing the molecular weight of the polymer. In fact, numerous studies indicate that increasing the molecular weight of the polymer increases craze strength, creep rupture strength, and endurance limit under cyclic loading conditions (Sauer and Richardson 1980; Hertzberg and Manson 1980; Argon 1989; Kramer and Berger 1990; Sánchez-Valencia et al. 2017). It is noteworthy to mention here that while amorphous polymers are more inclined towards crazing (which is a nanometer scale phenomena) under fatigue loads, semi-crystalline polymers tend to exhibit fibrillation (which happens to be more of a sub-micron scale event) as the primary mode of fatigue failure.

As mentioned above, semicrystalline polymers, on the whole, provide improved fatigue resistance over glassy amorphous polymers. One premise is that the composite, two-phase structure, consisting of crystalline and amorphous constituents, offers enhanced toughness. Improved yield strength is provided by the crystalline phase and ductility is provided by the compliant amorphous phase (generally above its glass transition temperature) along with post-yield mechanisms for lamellar plasticity.

### 2.4.2 The Effect of Reinforcements

The most common reinforcements for polymers include rubber particles, glass spheres, organic fillers, and fibers (continuous and chopped). Fibers have long been used to strengthen polymer resins and many composites offer enhanced mechanical attributes including increased elastic modulus, fatigue resistance, and fracture toughness. Composites provide a milieu of toughening mechanisms through crack bridging, fiber pull-out, kink-banding, and crack-tip shielding processes (Lang et al. 1984; Teoh 2000; Mortazavian and Fatemi 2015).

Organic fillers are often used to enhance tribological characteristics or to enhance thermal properties of the polymer; yet many of these systems benefit from augmented fatigue resistance through crack deflection processes. The presence of rubber particles can initiate a process-zone shielding mechanism involving massive shear banding of the matrix and leading to improved fatigue crack propagation resistance. The role of crack-tip shielding mechanisms on the crack growth rate regime has been modeled previously (Ritchie 1988). According to this model, the occurrence of a process-zone shielding mechanism should change the slope *m* in the Paris regime but should not affect crack growth behavior in near-threshold regimes. Experimental support of this model in polymers has also been given (Azimi et al. 1996) by demonstrating that the fatigue crack propagation characteristics are strongly influenced by the size of the rubber particles as well as the blend morphology.

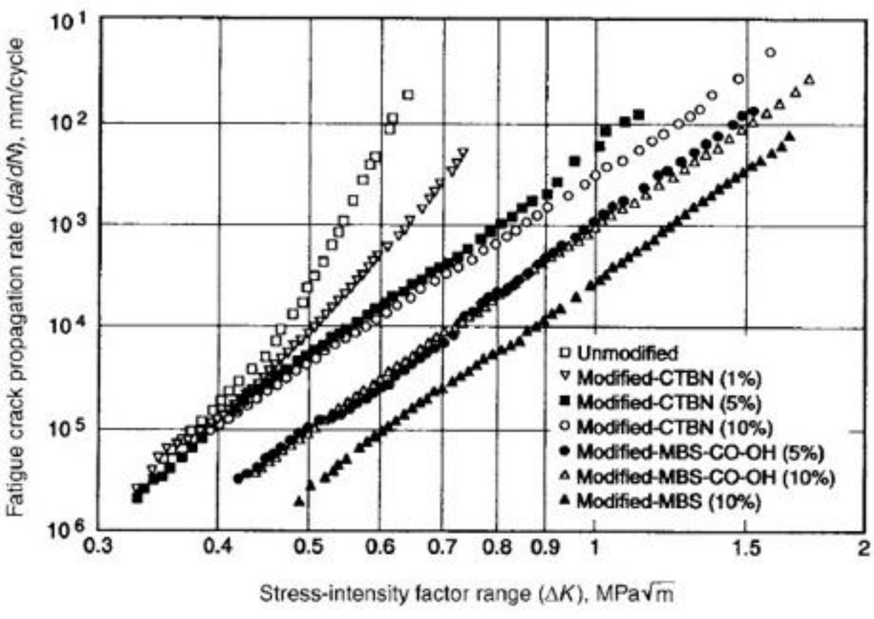


**Figure 7** Fatigue crack propagation plot which shows that the addition of rubber decreases the slope, *m*, and retards crack growth at high crack growth rates (Azimi et al. 1996).

Figure 7 reveals that the addition of rubber in epoxy decreases the slope, *m*, and retards crack growth at high crack growth rates, thereby establishing that the modifiers' volume fraction can affect the Paris regime. Nonetheless, the power law remains independent of the particle size and blend morphology for this polymeric system. It is noteworthy that at low values of stress-intensity range, where the process zone in front of the crack tip is small, the crack growth rates for these rubber-toughened epoxies are nearly identical to the neat resin. In this realm, the rubber reinforcements are not highly stressed and crack growth occurs with minimal plasticity. The mechanism changes at higher $\Delta K$ levels where the process zone becomes larger than the size of the particles. Within this highly stressed region, particle cavitation causes significant plasticity in the matrix and the crack propagation rate is reduced.

A study has shown that glass-filled, rubber-toughened blends offer improvements to fatigue crack growth resistance in epoxy resins (Azimi et al. 1996). It is believed that the improved fatigue crack propagation resistance is the result of a synergistic interaction between the hollow glass filler at the crack tip and the plasticity triggered by the presence of rubber particles. In the process of cavitation, the creation of new surfaces dissipates energy from the crack tip. This process is thought to relieve the triaxial state of tension existing in the matrix in the vicinity of the rubber particles, leading to a local state of plane stress and an increased plastic zone size (Yang and Liu 2001). Cavitation is not without mechanical penalty to these polymer systems as void formation promotes debonding between the rubber particles and the matrix.

The effect of carbon nanotube (CNT) inclusion on total life fatigue behavior of polyurethane (PU) composites has been studied extensively (Loos et al. 2013). It was found that the incorporation of CNTs increased the fatigue life of PU in the high-stress amplitude (low-cycle regime) by up to 248%. An interesting observation in reinforced polymers is that the second phase addition typically improves resistance to crack propagation; yet these same polymer systems can exhibit a decreased resistance to fatigue crack initiation or flaw inception. The second-phase addition serves as a nucleation site for crazes, voids, or shear bands and these mechanisms dissipate energy away from an advancing crack but serve as flaw initiation sites. An increased resistance to crack propagation but a degraded resistance to crack inception in rubber-modified polystyrene when compared to the unmodified resin has also been noted (Hertzberg and Manson 1980).

Reinforcements such as carbon-fibers are usually beneficial for enhancing the fatigue crack propagation resistance of polymers; yet, it has been found that this principle does not apply universally to all polymers. For instance, owing to poor interfacial adhesion, carbon-fiber reinforced UHMWPE performed poorly under *in-vivo* cyclic loading conditions in comparison to unmodified UHMWPE (Connelly et al. 1984; Wright et al. 1988; Medel et al. 2009). The choice of the reinforcement-matrix couple and interfacial bond strength greatly affect fatigue resistance of polymers. Thus, designers need to have a clear understanding of the component design and loading environment when making their polymer selection.

### 2.4.3 Viscoelastic Effects

Most polymers are viscoelastic, and a portion of their strain energy is dissipated under cyclic loading conditions in the form of heat generation. A consequence of hysteretic heating is that the specimen temperature increases until the heat generated per cycle is equal to the heat dissipated through mechanisms of conduction, convection, and radiation. The amount of temperature elevation depends strongly on the frequency of the test, the amplitude of the applied stress or strain, and the damping properties of the polymer. This is especially predominant in unnotched specimens, where the temperature of the polymer specimen can locally surpass the glass transition or the flow temperature of the polymer. The energy dissipated per second, $\dot{E}$, is given as (Ferry, 1961):

$$\dot{E} = \pi \nu J''(\nu, T, \sigma)\, \sigma^2 \qquad \text{Eq. [17]}$$

where $\boldsymbol{\nu}$ is the frequency, $J''$ is the loss compliance, and $\boldsymbol{\sigma}$ is the peak stress of the fatigue cycle. The rate of change of temperature for adiabatic heating conditions in which the heat generated is transferred into temperature rise is given as:

$$dT/dt = \dot{E} / \rho\, c_p \qquad \text{Eq. [18]}$$

where $\rho$ is the mass density and $c_p$ is the heat capacity of the polymer. As a general rule, the increase in temperature is proportional to the increase in frequency, stress amplitude, and internal friction of the polymer (Movahedi-Rad et al. 2019). In many polymer systems, the thermal work brought about by high damping and low thermal conductivity contributes to micro-mechanisms of permanent deformation, including craze formation, shear bands, voids, or even microcracks. The temperature rise in the specimen can be monitored with a thermocouple or an infrared sensor and many researchers limit test frequency or impose external cooling mechanisms to limit thermally driven fatigue mechanisms.

Under cyclic loading conditions, dissipative losses in viscoelastic polymers appear as hysteresis loops and provide useful insight into the micro-mechanisms of fatigue damage.

Figure 8 shows the hysteresis loops after various numbers of fatigue cycles in both high-impact polystyrene (HIPS) and acrylonitrile butadiene styrene (ABS). A distinction can be made between the two polymer systems, owing to differences between micro-mechanisms of deformation. In the ABS polymer blend, the hysteresis loops are symmetrical through the compression–tension cycle, while in HIPS, the hysteresis loops become much larger for the tensile portion of the fatigue cycle as the fatigue test progresses. These events are rationalized by the fact that ABS undergoes shear-yielding mechanisms, while the HIPS undergoes crazing, which requires a tensile component of stress. Crazing results from the fibrillation or polymeric drawing ahead of the fatigue flaw. The advancement of the craze zone is associated with damage accumulation in the leading fibrils and thus, the tensile portion of the hysteresis loop grows as damage accumulates in the specimen.

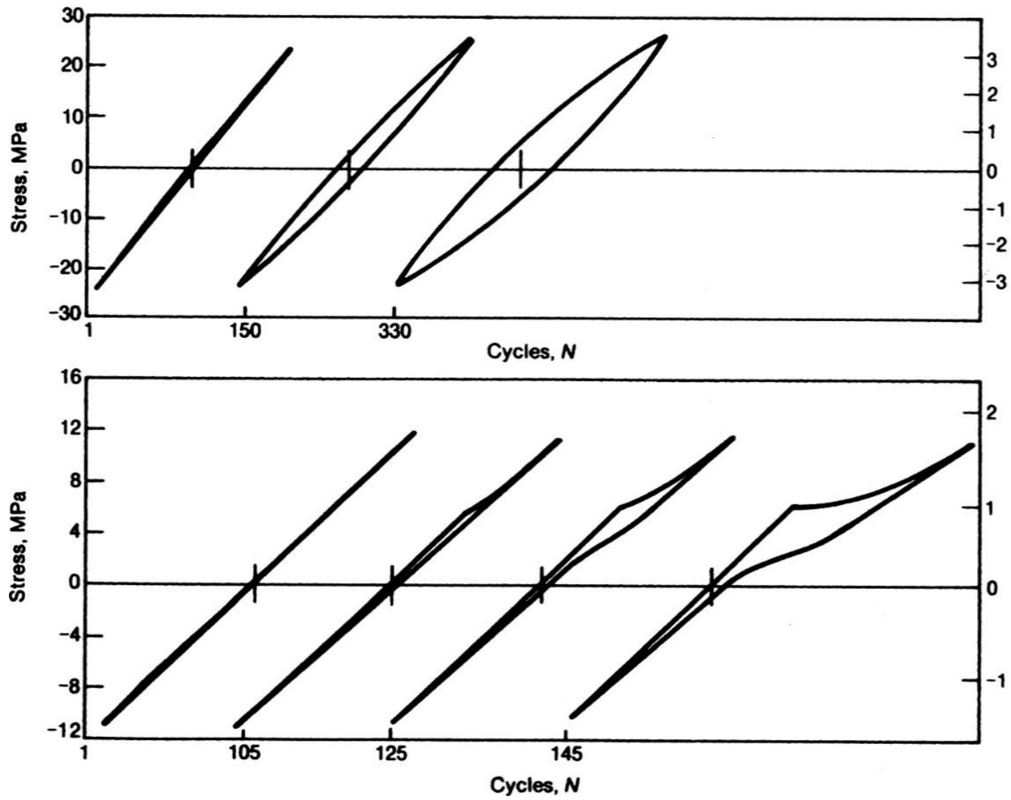


**Figure 8** Hysteresis loops after various numbers of fatigue cycles in both high impact polystyrene (HIPS) (bottom) and acrylonitrile butadiene styrene (ABS) (top). Note the lack of symmetry in the HIPS due to crazing mechanisms (Hertzberg and Manson 1980).

### 2.4.4 Mean Stress Effects

The fatigue response of a polymeric material is highly sensitive to the mean stress of the fatigue cycle. An interesting finding for engineering polymers is that, depending on the structure of the polymer and the micro-mechanisms of deformation, there are two distinct responses to an increase in mean stress. For a nominal stress-intensity range, certain classes of polymers exhibit an increase in crack propagation rate, while others show a decrease in crack growth rate. The published research on the effects of mean stress and R-ratio covers a broad range of polymer classes, including amorphous, semicrystalline, crosslinked, and rubber-modified polymers (Pruitt et al. 1992; Pruitt 1993; Pruitt and Suresh 1994; Pruitt and Rondinone 1996; Mukherjee and Burns 1971; Zhou and Brown 1992; Arad et al. 1971; Moskala 1991; Argon and Cohen 1990; Manson et al. 1981; Takemori 1982; Mills and Walker 1976; Scholz et al. 2018; Amjadi and Fatemi 2020; Klimkeit et al. 2011; Zheng et al. 2019). Table 1 provides a summary of the effect of mean stress for several polymers.

**Table 1** Effect of increasing mean stress on polymer fatigue behavior.

| |
|---|
| **Increasing crack propagation rate with increasing mean stress** |
| High-density polyethylene |
| Nylon |
| High-molecular-weight PMMA |
| Polystyrene |
| Epoxy |
| Polyethylene copolymer |
| UHMWPE |
| |
| **Decreasing crack propagation rate with increasing mean stress** |
| Low-density polyethylene |
| Polyvinyl chloride |
| Low-molecular-weight PMMA |
| Rubber-toughened PMMA |
| High-impact polystyrene |
| Acrylonitrile-butadiene-styrene |
| Polycarbonate |
| Toughened Polycarbonate Polyester |

The fatigue crack growth rates could be scaled to the stress-intensity factor with the following relationship (Arad et al. 1971):

$$da / dN = \beta \lambda^n = \beta (Kmax^2 - Kmin^2)^n \qquad \text{Eq. [19]}$$

where $\beta$ depends on the loading environment, frequency, and material properties, $n$ is a material constant, and $\boldsymbol{\lambda}$ is a parameter dependent on $K_{mean}$ and $\Delta K$. A micro-mechanistic explanation for this response to an increase in stress ratio or mean stress is also possible. Polymers that become more prone to fracture with increasing mean stress are most likely to be affected by the monotonic fracture process associated with the maximum portion of the loading cycle as it approaches a critical stress-intensity level. In general, these polymers are susceptible to crazing, chain scission, or crosslink rupture. For these polymer types, an increase in mean stress results in faster crack propagation rates as seen in polymers such as HDPE, Nylon, epoxies and PS.

Several polymers offer improved resistance to crack propagation as the mean stress is increased, for instance, such phenomenon is observed in LDPE, PVC, HIPS, ABS, PC, and toughened PC. Many of these polymeric systems also demonstrate a marked improvement of fracture toughness with increasing mean stress (Hertzberg and Manson 1980). They postulated that the strain energy normally available for crack extension is consumed through deformation or structural reorganization ahead of the crack tip. The use of strain energetics to describe fracture processes in polymers is formulated as (Andrews 1969; Manson et al. 1981):

$$T = T_o\, [\, C / (C - f(\Psi))]$$ Eq. [20]

where $T$ is the total energy used by the polymer to create a new unit area of surface through crack advance, $T_0$ represents the elastic strain energy, $C$ is a material constant that depends on the strain state of the polymer, and $\Psi$ is the hysteresis ratio. Here, $\Psi$ captures the energy lost due to inelastic energy expenditure. If the energy loss is large, the amount of energy needed to cause fracture increases. Thus, the crack growth rate is reduced with increasing $\Psi$. Moreover, the effect of mean stress on the fatigue crack propagation resistance of the polymer is directly linked to the parameter $\Psi$. Hence, polymers with a molecular structure susceptible to hysteretic losses, or capable of structural reorganization, are likely to be more resistant to fatigue crack propagation as the mean stress is increased. These polymers have near-tip processes that dissipate elastic energy ahead of the crack tip.

### 2.4.5 Variable Amplitude Effects

The effect of variations in the load cycle can have a profound effect on polymeric materials (Mars and Fatemi 2004; Teoh 2000). Understanding the variable amplitude behavior is also important for the design of polymeric components where stresses are expected to vary throughout the life of the device. Additionally, this is a concern for components that are likely to experience tensile or compressive overloads, and such effects are quite prevalent in the sporting and orthopedics applications of polymers. It is common to model the effect of variable amplitude loading using a cumulative damage approach, whereby the Palmgren-Miner's rule (Miner 1945; Palmgren 1924) is employed to predict the life of the device. The incremental damage $d_i$ accrued owing to a certain stress amplitude $\boldsymbol{\sigma}_i$ is formulated as

$$d_i = N_i / N_{fi}$$ Eq. [21]

where $N_i$ is the number of cycles experienced with stress amplitude $\boldsymbol{\sigma}_{\mathrm{i}}$ and $N_{fi}$ is the number of cycles to failure if only $\boldsymbol{\sigma}_{\mathrm{i}}$ was applied from start till end when the sample finally fails due to fatigue. Hereafter, the total damage $D$ can be ascertained by summing all these individual incremental damages as formulated below-

$$D = \Sigma\, d_i = \Sigma\, N_i / N_{fi}$$ Eq. [22]

It should be noted here that the total damage $D$ a material can sustain until fatigue failure is always 1.0.

Nevertheless, the aforementioned approach predicated on damage accumulation cannot capture the subtle effects of the nature (compressive or tensile) or position of the overload in the loading sequence, and its subsequent effect on a propagating crack. For example, it is well known that the application of a single tensile overload can extend the life of a cracked component by retarding the rate of crack advance (Suresh 1998). This transitory behavior is often dictated by several mechanisms including crack closure (Elber 1970), residual compressive stresses (Suresh 1983;

Pruitt and Suresh 1993), and crack tip blunting (Rice 1967). Crack closure justifies the retardation of crack velocity in terms of residual compressive stresses left in the plastically deformed wake of the advancing crack. This results in premature contact between the crack faces while the specimen is still in the tensile portion of the fatigue cycle. Crack closure effectively reduces the stress-intensity range driving the crack advance. This mechanism has been initially proposed to describe crack retardation in PMMA (Pitoniak et al. 1974) and PC (Murakami et al. 1987). Blunting has been proposed by others to describe the reduced crack velocity following tensile overloads (Banasiak et al. 1977). Although crack-tip blunting can affect the crack velocity subsequent to the overload, it does not provide a basis for the prolonged regime of crack retardation. The zone of residual compressive stresses sustained at the crack tip upon unloading in amorphous polymers increases in size and magnitude as the far-field tensile load increases (Pruitt and Suresh 1994). These residual compressive stresses sustained at the crack tip are believed to decrease the crack propagation rate following the tensile overload. The crack has to then grow through this zone of enhanced residual compression before it can return to its initial crack propagation rate for the $\Delta K$ sustained prior to overload. Many current life-prediction models are formulated based on residual compressive stresses for the rationalization of crack retardation effects.

### 2.4.6 Waveform and Frequency Effects

Many polymers, due to their viscoelastic nature, are highly sensitive to the waveform or frequency of cyclic loading (Eftekhari and Fatemi 2016; Mars and Fatemi 2004). For instance, some crazeable polymers such as PS, PMMA, and HIPS exhibit decreased crack propagation as the test frequency is increased, while materials such as PC, nylon, and polysulfone exhibit no sensitivity (Hertzberg and Manson 1980). In such polymers, the increased test frequency can diminish chain disentanglement effects at the crack tip, resulting in a reduction in the rate of crack advance.

Crack propagation in a polymer could be described as the sum of the elastic and viscoelastic contributions (Wnuk 1974):

$$da/dN = C_1\,(\Delta \mathrm{K}/K_{IC})^{n_1} + C_2\left(\Delta \mathrm{K}/K_{IC}\right)^{n_2}\left(\frac{1}{v}\right) \qquad \text{Eq. [23]}$$

where the first term is the elastic contribution, and the second term is the time-dependent contribution (viscoelastic component) and includes a creep compliance term, $C_2$, and the test frequency, $\boldsymbol{\nu}$.

The strain rate can also play a critical role in the fatigue response of time-dependent polymers. Strong sensitivity to the waveform parameter was found in several polymers such as PVC, PS, PMMA, and vinyl urethane (VUR) (Hertzberg et al. 1975). For instance, the square wave provides a high strain rate in ramp up and then subjects the specimen to a longer period of peak load than a triangular waveform with the same stress amplitude. The difference in load function can cause major differences in fatigue crack propagation (FCP) behavior. For example, the fatigue crack propagation rate in VUR is reduced by nearly an order of magnitude when changing from a triangular to a square wave loading function (Harris and Ward 1973). This behavior is attributed to the higher strain rate that dominates in the case of very flexible polymers, such as VUR. Another important factor is the amount of creep sustained in the peak loading portion of the fatigue cycle. Consequently, polymers that are susceptible to creep damage will generally perform poorly when tested under the square waveform loading due to creep at peak load (Harris and Ward 1973).

### 2.4.7 Environmental Factors

Environmental factors play a critical role in the fatigue performance of engineering polymers (Teoh 2000; Scholz et al. 2018). Such factors can include ambient temperature, chemical environment, exposure to ionizing radiation, oxidative embrittlement, or stress cracking. The ambient temperature relative to the glass transition temperature ($T_g$) is important for predicting how the polymer is going to behave. At temperatures above $T_g$, many polymers will be susceptible to viscous effects. Well below $T_g$, the polymers will behave in a glassy manner. The chemical environment surrounding the polymer is also of paramount importance. Many ester-based polymers undergo scission in aqueous environments, while others are affected by the environmental pH. Some amorphous polymers are known to be susceptible to chemically induced crazing (Hertzberg and Manson 1980). In such cases, the crack inception values can be substantially reduced in the presence of aggressive media (Hertzberg and Manson 1980). For example, PC is known to nucleate surface crazes in the presence of acetone vapor. Many rubbers are susceptible to oxidation-induced embrittlement (Kurtz et al. 1994). Many medical polymers, such as orthopedic grade UHMWPE or bone cement (PMMA), degrade due to oxidation embrittlement and chain scission. These degradative mechanisms are induced by ionizing modes of sterilization and subsequent aging (Dawes and Glover 1996; Kurtz et al. 1994; Connelly et al. 1984; Wright et al. 1992; Goldman and Pruitt 1998; Goldman et al. 1998; Rimnac et al. 1988). In order to accurately predict the fatigue behavior of polymers, fatigue tests must closely mimic not only the stress variations but also the chemical and aging environments that are most likely to be encountered in the device's lifetime.

A compilation of several key studies which investigated the fatigue characteristics of different polymers and polymer composites has been presented in Table 2.

**Table 2** Novel polymer fatigue studies (2009–2016)

| Researcher | Key research takeaways |
|---|---|
| Krause 2016 | Characterized epoxy resin system Araldite LY564/Aradur22962 and proposed a novel physically based fatigue failure criterion for polymers under multiaxial loading. |
| Kanters et al. 2015 | Compared and contrasted the compliance method with that of optical tracking method of fatigue crack propagation in polymers and it was reported that the nonlinear and viscoelastic behavior of polymer proves to cause a strong loading condition and time dependency of calibration curve and as a result no unique relation could be found for crack length as a function of dynamic compliance. |
| Garcea et al. 2015 | Studied the fatigue behavior of toughened and untoughened matrices. It was found that for the toughened systems, damage does not propagate evenly and in contrast untoughened material is characterized by more uniform crack progression. |
| Garcea et al. 2014 | Evaluated fatigue damage micro-mechanisms in [90/0]s carbon fiber reinforced epoxy double-edge notched specimens using in situ synchrotron radiation computed tomography and the damage was found to be quantified in terms of crack opening and shear displacements. |

| | |
|---|---|
| Klimkeit et al. 2011 | Conducted an experimental evaluation of the multiaxial fatigue behavior of PBT–PET GF30 (polybutylene terephthalate–polyethylene terephthalate with 30% mass short glass fibers) and PA66 GF35 (Polyamide 66 with 35% mass short glass fibers) under constant amplitude force loading and analyzed the experimental results using a through process modeling. |
| Berrehili et al. 2010 | Explored the multiaxial fatigue behavior of polypropylene pipes under tension and fatigue loadings. A multiaxial fatigue criterion was proposed and it depicted that the fatigue behavior of semi-crystalline polymer seems to be governed by the von Mises maximum stress. |
| Charles et al. 2010 | Investigated the Rolling Contact Fatigue (RCF) behavior of polyamide 6 nanocomposites. RCF behavior at different normal loads (P) (150, 175, 200, and 225 N) and rolling speeds (V) (1000, 1500, and 2000 rpm) was investigated to understand the pressure–velocity (PV) parameter effects. It was found that the RCF life of PA 6 organo-clay reinforced nanocomposite is the function of rolling speed and applied load. |
| Tao and Xia 2009 | Probed the biaxial fatigue behavior of an epoxy polymer under cyclic shear and proportional axial-shear combined loadings with mean strains and multiaxial fatigue life prediction models were established upon stress-, strain-, and energy-based approaches with consideration of mean stress/strain effect, where better agreement was achieved in stress-based and energy-based approaches. |
| Zenkert and Burman 2009 | Carried out quasi static tests in tension, compression, and shear on a closed cell foam of poly-metacrylimide (Rohacell) with three different densities. It was found that the fatigue life for different load types exhibit different failure mechanisms. |

## 2.5 Concluding Remarks

The fatigue performance of engineering systems that incorporate polymeric constituents is quite complex. Many theoretical models exist which can be utilized for attaining a reasonable estimate of the fatigue life without conducting prolonged experiments. These include the total-life and the defect-tolerant philosophes. The total-life philosophy is generally employed to predict the fatigue life of a polymeric component that is likely to be free of significant defects or stress concentrations and that is expected to spend the majority of its lifetime in the initiation stage of crack growth. In contrast, the fracture mechanics approach adopted in the defect-tolerant philosophy is used for fatigue prediction of polymeric structural components that have initial flaws or significant stress concentrations and which are likely to sustain a large degree of stable crack growth prior to fracture. However, these models have a lot of underlying assumptions which might not necessarily hold true during the entire service life of an actual polymeric component. For instance, the fatigue characteristics of polymers are affected by not only mechanical variables but also microstructural attributes, as well as the intricacies of the fatigue test. For safe design of polymeric devices, it is imperative that appropriate test conditions are used that best mimic the service conditions of the component under investigation. Parameters like frequency, strain rate, waveform, temperature, and environment can impact fatigue behavior. Similarly, tests should utilize specimens with a structural composition that replicates the polymeric component as molecular factors such as molecular weight, crystallinity, and crosslinking strongly influence fatigue micro-mechanisms. This chapter compiles the relevant literature, encompassing both the classical studies as well as the relatively new findings pertaining to the fatigue of polymers and is intended to assist researchers, designers, and technical professionals by acting as a centralized repository on polymer fatigue behavior.

# Chapter 3 –Study of crack initiation phenomena in orthopedic grade UHMWPE from clinically relevant notches: Preliminary Findings

*This chapter has also been included published as part of a PhD dissertation titled Study of the Bio-Tribo-Mechanical Characteristics of Orthopedic-Grade Polymers (Roy 2024).*

### 3.1 Introduction

Total joint replacement (TJRs) is one of the solutions for a severely degraded osteoarthritic joint such as the hip, shoulder, or knee ("5 Ways to Manage Arthritis | CDC" 2023). TJRs impart relief from pain and much-needed mobility to osteoarthritis-afflicted patients. A specialized polymer called Ultra-high molecular weight polyethylene (UHMWPE) is used as the bearing material in TJRs and has been in use since the 1960s (Charnley 1961; S. M. Kurtz 2009). The choice of UHMWPE arises from a volley of attributes including but not limited to wear resistance, energetic toughness, and biocompatibility.

Despite its excellent bio-tribo-mechanical performance, UHMWPE is subjected to large cyclic contact stresses and must endure loading for 20-30 million cycles in-vivo. Such extensive biomechanical demand can result in the generation of sub-micron sized wear debris, ultimately leading to osteolysis, implant loosening, and failure of the TJR. There is an ongoing effort to develop formulations of UHMWPE that resist the troika of challenges faced in the body – wear, fatigue, and oxidation (Atwood et al. 2011; S. M. Kurtz and Oral 2016; Ansari, Ries, and Pruitt 2016). The optimal microstructure remains that of moderately cross-linked UHMWPE which has been remelted alongside vitamin E added to protect it from oxidation while balancing fatigue and wear properties (Atwood et al. 2011; Bracco and Oral 2011).

### 3.2 Background

Fatigue behavior can be divided into two categories, namely, fatigue crack initiation and fatigue crack propagation. The latter has been extensively studied and there is a plethora of crack propagation studies which have comprehensively characterized UHWMPE (Ansari, Ries, and Pruitt 2016; L. Pruitt, Wat, and Malito 2022; Furmanski and Pruitt 2007; Patten et al. 2011a; Ansari et al. 2016; Furmanski and Pruitt 2018; Baker, Hastings, and Pruitt 1999; 2000; Baker, Bellare, and Pruitt 2003; Bradford et al. 2004; L. A. Pruitt et al. 2005; Ries and Pruitt 2005; Simis et al. 2006).

One approach to study the fatigue life of a polymer component is using the defect-tolerant philosophy which utilizes the fracture mechanics formulation to assess the crack growth dynamics. Numerous studies report the steady-state crack propagation in the Paris regime in the form of da/dN vs $\Delta K$ curves across clinically relevant formulations of UHMWPE. When it comes to the study of crack growth initiation, researchers have reported crack initiation in terms of $\Delta K_{inception}$ which is the minimum stress intensity that needs to be applied for the crack to propagate at the rate of $10^{-6}$ mm/cycle (Baker, Bellare, and Pruitt 2003; Simis et al. 2006). Exacerbating the problem is the insight into the crack propagation behavior that cracks, once initiated, can propagate under static and/or marginal or no stress fluctuations, with the crack propagation being dependent primarily on the peak stress intensity and not the stress intensity range (Furmanski and Pruitt 2007; 2018; P. A. Sirimamilla, Furmanski, and Rimnac 2013; 2011). This implies that a concerted effort needs to be made towards precluding the nucleation/ initiation of cracks so that the subsequent issues with propagation never transpire.

Another approach is the total life fatigue data whereby the S-N route (stress amplitude vs number of cycles) is adopted and formulated using the Basquin relation (Baker, Bellare, and Pruitt 2003; Michael C. Sobieraj et al. 2013). Total life philosophy presumes that the fatigue life is a sum of the time/cycles to initiate a flaw and the time/cycles for it to grow to a critical crack size. For fatigue-brittle polymers, the first component is rather predominant, implying that the time/cycles to nucleate a flaw (crack) is substantially higher than the time/cycles for it to grow to a critical size and for fatigue failure to ensue. Therefore, it is safe to presume that once a flaw initiates, that can be approximated to be the fatigue life of the specimen, ignoring the second component. That underscores the importance of crack initiation studies. These are usually conducted in the classic S-N style format by loading specimens at constant-amplitude stresses and observing when the specimen fails.

It is of paramount importance to factor in notches and their effects on the fatigue behavior of medical-grade polymers like UHMWPE. The reason to focus on notches can be traced back to the design of TJRs which have stress-concentration features (posts, undercuts, grooves as well as various locking mechanisms) by virtue of their clinical requirements. These regions of heightened stress-concentrations often act as sites of crack initiation from which fatigue cracks then propagate through the material, leading to the catastrophic failure of the TJR inside the patient (Furmanski et al. 2009; Furmanski, Kraay, and Rimnac 2011).

In one study, fatigue testing was conducted using cylindrical dog-bone specimens with notches present centrally while a smooth cylindrical geometry was the control sample (Michael C. Sobieraj et al. 2013). Their experimental results demonstrated that conventional UHMWPE (ram extruded GUR 1050, sterilized at 30kGy in inert nitrogen environment) strongly follows the S-N curve-based Basquin relation but for other formulations of UHMWPE (such as moderately or highly cross-linked) with notches, the results exhibit significant variance in their S-N distribution data or don't follow the Basquin relation at all. On the other hand, another study also used small dog-bone specimens for their fatigue behavior investigation but had no notches machined into the samples (Baker, Bellare, and Pruitt 2003). Both of the aforementioned studies also had varying definitions for the N value (number of cycles) as one of them used the number of cycles to the onset of yielding (Baker, Bellare, and Pruitt 2003) while the other opted for fracture (Michael C. Sobieraj et al. 2013) as the definition of failure of the specimens. The current study is predicated on the initiation of crack(s) at/near the vicinity of the notch root as the failure criteria but given the very marginal difference between $N_{initiation}$ and $N_{failure}$, the N value is experimentally determined as the number of cycles to fatigue failure incorporating both the predominant initiation plus the numerically insignificant propagation cycles. Moreover, while both studies (Baker, Bellare, and Pruitt 2003; Michael C. Sobieraj et al. 2013) incorporated different formulations of UHMWPE, neither utilized the current-day vitamin E-added formulation for their fatigue tests in the presence of notches, which is one of the material groups explored in the current work.

Other peripheral studies conducted by groups investigating fatigue of UHMWPE contributed to better comprehension of the effects of notches and varied notch root radii. For instance, Rimnac and co-workers found that the axial yield stress increased in the presence of notches incorporated into the tensile specimens while observing a reduction in the ultimate properties (both stress and strain) vis-à-vis unnotched specimens and reported a 'notch-strengthening and hardening' phenomenon that depended on the severity of the notching (Michael C. Sobieraj et al. 2013; M. C. Sobieraj, Kurtz, and Rimnac 2005; Michael C. Sobieraj et al. 2008). This was attributed to the triaxial state of stress that exists in the region surrounding the notch in comparison to the uniaxial state of stress observed in unnotched specimens. Typically, fracture in UHMWPE starts with microvoids coalescing into a 'crack', followed by slow fracture up until it reaches a critical dimension after which fast fracture occurs (Gencur, Rimnac, and Kurtz 2003). This is the case for unnotched specimens where a standard axial force is applied. However, as the state of stress transforms to a triaxial one in the presence of notches, it inhibits chain alignment and subsequently, the cascade of void formation, coalescence, and crack growth to fast fracture is interrupted (M. C. Sobieraj, Kurtz, and Rimnac 2005). It is pertinent to mention here that just like notches culminate in a triaxial state of stress and inhibit chain alignment, crosslinking of UHMWPE also has a similar microstructural effect on the lamellar alignment prevention (Klapperich, Komvopoulos, and Pruitt 1999; Zhou and Komvopoulos 2005). The key takeaway is that geometric features like notches significantly modify the micro-mechanisms of void formation and crack growth to fracture, and drastically reduce the critical stress intensity or threshold needed for failure. These findings have strong implications for the notch-based fatigue tests and interpretation of the results obtained therein.

While it is known that cracks in UHMWPE can propagate once initiated, under static loads with minimal or no fluctuations (Furmanski and Pruitt 2007), it is even more concerning to learn that cracks can initiate under static loads from notches in UHMWPE of similar root radius as the design features (like fillets) inherently present in TJR components (P. A. Sirimamilla, Furmanski, and Rimnac 2011; 2013). Crack initiation under quasi-static loads was preceded by non-uniform material de-cohesion at the notch surface followed by a tortuous crack front, after which the crack propagated at velocities that could be correlated to the magnitude of static loads being applied to the compact tension samples, hereafter referred to as C(T) samples. Single-layer and multi-layer crack initiation was also noted. The former occurred when the crack front erupted on the line of the notch root while the latter was seen in some cases whereby the crack initiated simultaneously at multiple parallel planes in the vicinity of the notch root. A positive correlation was obtained between the time for crack initiation and the type of crack initiation, i.e. single-layer or multi-layer, and the time for crack initiation also correlated with the distance between the different layers in the multi-layer crack initiation. Furthermore, increased crosslinking (a product of increased gamma radiation dosage) was found to reduce the crack initiation resistance and detrimentally increase the crack propagation velocities. Noteworthy to mention here that the researchers behind these studies employed a video measurement apparatus and quantified crack initiation in terms of initiation time ($t_i$) and proved that the viscoelastic fracture model developed by Williams (Williams 1977) can be successfully used to predict crack initiation in crosslinked formulations of UHMWPE.

A parametric study demonstrated the relationship between notch root radii and the crack initiation dynamics under quasi-static loading conditions (P. A. Sirimamilla, Rimnac, and Furmanski 2018). Two highly cross-linked formulations of UHMWPE and three different notch root radii were included in the scope of this investigation and it again went to prove that the Williams' viscous fracture model (Williams 1977) governs crack initiation in these UHMWPE formulations. Reaffirming previous results, this study again evinced that increased crosslinking density resulted in decreased crack initiation resistance in the presence of notches. Therefore, increasing crosslinking density reduced the resistance to fracture for UHMWPE, given the quasi-static nature of the loads. For the sharp notch case, crack initiation was almost instantaneous for all the static loads that were applied in those experiments but for the same static loads, the blunter the notch (larger notch root radii) the longer it took to initiate a crack. This has been explained using the Williams fracture model whereby the $J_0$ (energy available at the notch front) is substantially reduced in the case of the blunter notches, making it harder to initiate a crack front from the notch tip. In addition, the work specified that a decrease in the applied quasi-static load came with a concomitant increase in the crack initiation time.

While the previous parametric study explored the notch root radii effect on crack initiation under quasi-static loading conditions, a follow-up study expanded into the crack initiation dynamics under cyclic loading conditions for only one clinically relevant notch root radius (0.25 mm) in highly cross-linked and remelted UHMWPE (A. Sirimamilla and Rimnac 2019). Interestingly, for the same set of experimental parameters (such as same maximum load), the crack initiation time ($t_i$) decreased by an order of magnitude for the cyclic loading case vis-à-vis the static one. Additionally, cyclic loading parameters like frequency, loading rate, and waveform had a strong effect on crack initiation alongside the $J_0$ parameter. Unlike the previous study (P. A. Sirimamilla, Rimnac, and Furmanski 2018), no multi-layer crack initiation was detailed in their results.

The current study is predicated on pertinent research published a few years ago whereby crack propagation dynamics for cracks originating from notches of different root radii was probed using a linear-elastic fracture mechanics approach (Ansari et al. 2016). Three relevant UHMWPE formulations were considered: conventional UHMWPE, highly cross-linked and remelted UHMWPE, and vitamin E blended and highly cross-linked UHMWPE. The stress intensity factor K (driving force) is markedly influenced by the notch geometry, yet the inherent mechanisms driving crack growth in UHMWPE in the presence of notches are not significantly affected by whether the crack is propagating through the elasticity or plasticity-affected zones in the vicinity of the notch. Another key finding was that crack growth rate was irrespective of the notch root radii and that crack growth was predominantly determined by the microstructure of UHMWPE with highly crosslinked formulations exhibiting fast crack growth rates while the conventional UHMWPE showed the slowest. Therefore, crack growth dynamics weren't affected by notch geometry once a crack initiated. But then, crack initiation as a function of notch geometry becomes worthy of further enquiry. This forms the foundation of the current study.

Another point worthy of being noted here is that the former study purposefully added a razor-sharp crack edge at the notch root for ease of crack growth inception, which foregoes any significant finding from the crack initiation standpoint. Building on the insight of previous research, the present study examines crack initiation from the notched regions. Thus, cracks nucleate from inherent material flaws or machining features rather than any artificial interventions in this particular study.

### 3.3 Objectives

The current investigation presents some initial findings related to the effect of different notch root radii, UHMWPE formulations, as well as different a/W ratios on crack initiation phenomenon from clinically relevant notches. Different load amplitudes are applied on the samples, in essence, applying different stress intensities, and consequently, the number of fatigue cycles to crack initiation (experimentally measured here as fatigue failure) are noted. This chapter also includes failed endeavors as part of the study, which could potentially help future researchers as lessons learnt, for preparing their research plans to study crack initiation from clinically relevant notches in UHMWPE or other orthopedic-grade polymers in general.

### 3.4 Materials and Methods

Two clinically relevant notch root radii (0.25 mm and 3 mm) and two formulations, namely, virgin UHMWPE as well as 0.1 wt.% vitamin E-blended highly crosslinked UHMWPE, both derived from GUR 1020 resin originally, are included in the scope of this work. The former formulation is hereby referred to as UHMWPE and serves as the control group whereas the latter formulation with vitamin E and 100 kGy crosslinking dosage is referred to as VXLPE, following a convention set in a previous work (Ansari et al. 2016). C(T) samples were machined from blocks of UHMWPE and VXLPE sourced from Orthoplastics located in Lancashire, UK (Malito et al. 2018) and the dimensions were based on the recommendations from the ASTM Standard ASTM E647-15$^{€1}$ ("ASTM E647-15e1 - Standard Test Method for Measurement of Fatigue Crack Growth Rates" 2015; Patten et al. 2011b). It is important to state here that while ASTM E647 prescribes a set of dimensions and dimensional ratios and proportions for the specimens used for fatigue testing, the standard was originally developed keeping ductile metals and metallic alloys in mind. Consequently, some of the prescriptions do not necessarily translate to the polymer material class. This necessitates an upgrade to the ASTM E647 standard for ensuring that it can be meticulously utilized for fatigue testing of polymeric materials.

The following dimensions (all reported in mm unless specified otherwise) were chosen for the specimen geometry: W = 25, L = 31.25, h = 1.5, B = 5, $\phi$ = 6.25, initial notch length a = $a_n$ = 6.25, 8.75, 12.5, 15, and notch root radius $\rho$ = 0.25, 3. The other relevant dimensions have been labelled in the diagram below, all of which are based on the ASTM standard cited earlier. It is to be noted here that all dimensions remain the same as the ones reported in Figure 9 except the notch root radius $\rho$ varying between 0.25 and 3 mm (as marked on the figure) and also the initial notch length 'a' varying between 6.25 to 15 mm. The initial notch lengths were determined based on different a/W ratios of 0.25, 0.35, 0.5, and 0.6.

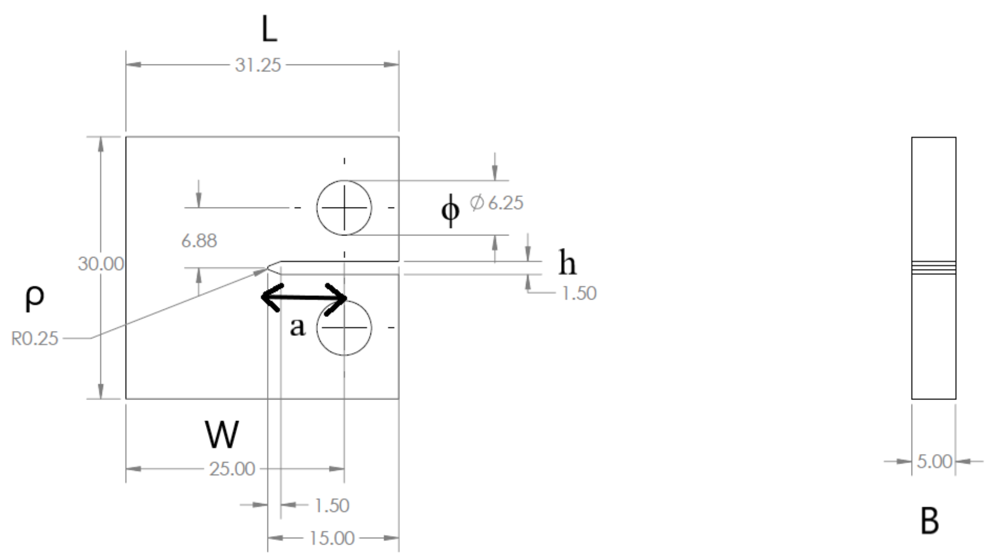


**Figure 9** Dimensions of a typical C(T) sample used for the crack initiation fatigue studies based on ASTM Standard ASTM E647-15€1. Dimensions shown are given in mm.

Tension-tension loading based fatigue tests were conducted on MTS Elastomer Test System Model 831 machine. The R-ratio was kept constant (R=0.1) across all fatigue experiments with the increasing loads adjusted accordingly. The following loads were used: 10-100N, 15-150N, 18-180N, 20-200N, 22-220N, 25-250N, 28-280N, 30-300N, and 80-800N. Fatigue tests were performed at room temperature using a load-controlled sinusoidal waveform applied at a frequency of 5 Hz. Additionally, an air coolant system was utilized to reduce the possibility of hysteretic heating (M. C. Sobieraj and Rimnac 2009). Tests were stopped at N = 25000 cycles periodically to inspect crack initiation on the notch surface or in its vicinity. The notch tip was examined using a Zeiss AX10 microscope with a magnification of 50x. If a crack didn't initiate after 25000 cycles, the loading was increased to the next step (say 20-200N followed by 22-220N and so on). This process of incrementally increasing the load after a preset number of cycles continued until the sample failed via fatigue failure. Any atypical deformation in the samples post-loading was also closely monitored and if found, the test was immediately discontinued. Two samples were tested for each material group and the details of the sample geometries, material formulation, test conditions, are comprehensively tabulated in Table 3.

The stress intensity values (ΔK) were calculated using the formulation provided in Equation A1.3 of the ASTM standard ("ASTM E647-15e1 - Standard Test Method for Measurement of Fatigue Crack Growth Rates" 2015), also stated below-

$$\Delta K = \left({\Delta P}/{B\sqrt{W}}\right)\left({2+\alpha}/{(1-\alpha)^{3/2}}\right)(0.886 + 4.64\alpha - 13.32\alpha^2 + 14.72\alpha^3 - 5.6\alpha^4) \quad \text{Eq. [24]}$$

Where ΔK is the stress intensity at the crack tip (notch root in this case), ΔP is the load applied, and B, W, and α = a/W are sample dimensions. Thereafter, ΔK values were plotted against the number of cycles to failure ($N_{failure}$) for samples P7-P10 which were only tested at the highest loads and were fatigued to failure therein. Samples P5 and P6 were deliberately removed from the analysis since these two samples were incrementally loaded and there isn't a way to merge the fracture mechanics-based ΔK values with the Palmgren-Miner's rule. These values of ΔK obtained from the study were then compared to $\Delta K_{threshold}$ values obtained from other experiments performed in a different unpublished study.

**Table 3** Compilation of fatigue crack initiation specimen- geometries, material formulations, test conditions, and results.

| Sample | Material | Cycles | Load in N | a/W ratio | Notch root radius (mm) | Final outcome |
|---|---|---|---|---|---|---|
| P1 | VXLPE | 6881 | 25-250 | 0.25 | Sharp notch tip | Sharp C(T) sample showed noticeable crack initiation of 0.198 mm within 6881 cycles |
| P2 | UHMWPE | 0 | 80-800 | 0.25 | 3 | Sample was loaded to setpoint (440N) and sample broke at one of the pin holes |
| P3 | UHMWPE | >35,000 | 30-300 | 0.25 | 3 | A crack didn't initiate at the notch, but the sample deformed at one of the holes |
| P4 | UHMWPE | >100,000 | 20-200 | 0.25 | 3 | No crack initiated on or in the vicinity of the notch |

| | | | | | | |
|---|---|---|---|---|---|---|
| P5 | VXLPE | 75000<br>50000<br>25000<br>50000<br>9315 | 18-180<br>20-200<br>22-220<br>25-250<br>28-280 | 0.35 | 0.25 | Sample broke into two parts at the highest load. |
| P6 | VXLPE | 340<br>117000<br>1561 | 10-100<br>15-150<br>20-200 | 0.5 | 0.25 | Sample broke into two parts at the highest load. |
| P7 | VXLPE | 86 | 20-200 | 0.6 | 0.25 | Sample broke into two parts at the highest load. |
| P8 | VXLPE | 3849 | 20-200 | 0.5 | 0.25 | Sample broke into two parts at the highest load. |
| P9 | VXLPE | 71 | 20-200 | 0.6 | 0.25 | Sample broke into two parts at the highest load. |
| P10 | VXLPE | 12539 | 28-280 | 0.35 | 0.25 | Sample broke into two parts at the highest load. |

### 3.5 Results and Discussion

This section includes the results from the initial trial and error with the fatigue testing parameters and C(T) specimen geometries, encompassing all the ‘failed’ tests (not to be confused with fatigue failure of a component) and the technical learnings along the way as well actual fatigue-failure results. The results are reported with the samples indexed as P1, P2…P10. Specifics of the sample geometry, loading conditions, and visuals of failures (or lack thereof) have been presented in Table 3 and figures in this section.

Figure 10 shows the samples P1-P4 after completion of testing. The red circles demarcate the area of interest where crack initiated (P1) or failure ensued (P2) or abnormal deformations were observed (P3). The instantaneous failure and abnormal deformations noticed in samples P2 and P3 respectively (both with a/W ratio of 0.25) provided impetus to discard this particular a/W geometry, course correct, and increase the a/W ratio and/or reduce the load. This was attributed to the stress-concentrations near the hole-notch interface regions that were causing the samples to fail upon loading or deform abnormally around that area. The load was reduced to 20-200N for P4, yet no crack initiated even after 100,000 cycles at which point the fatigue test was stopped. Therefore, a/W = 0.25 was proving to be detrimental to the sample geometry and reliable fatigue crack initiation data was not possible from the notches with lower loads or high notch root radius (at this specific a/W ratio).

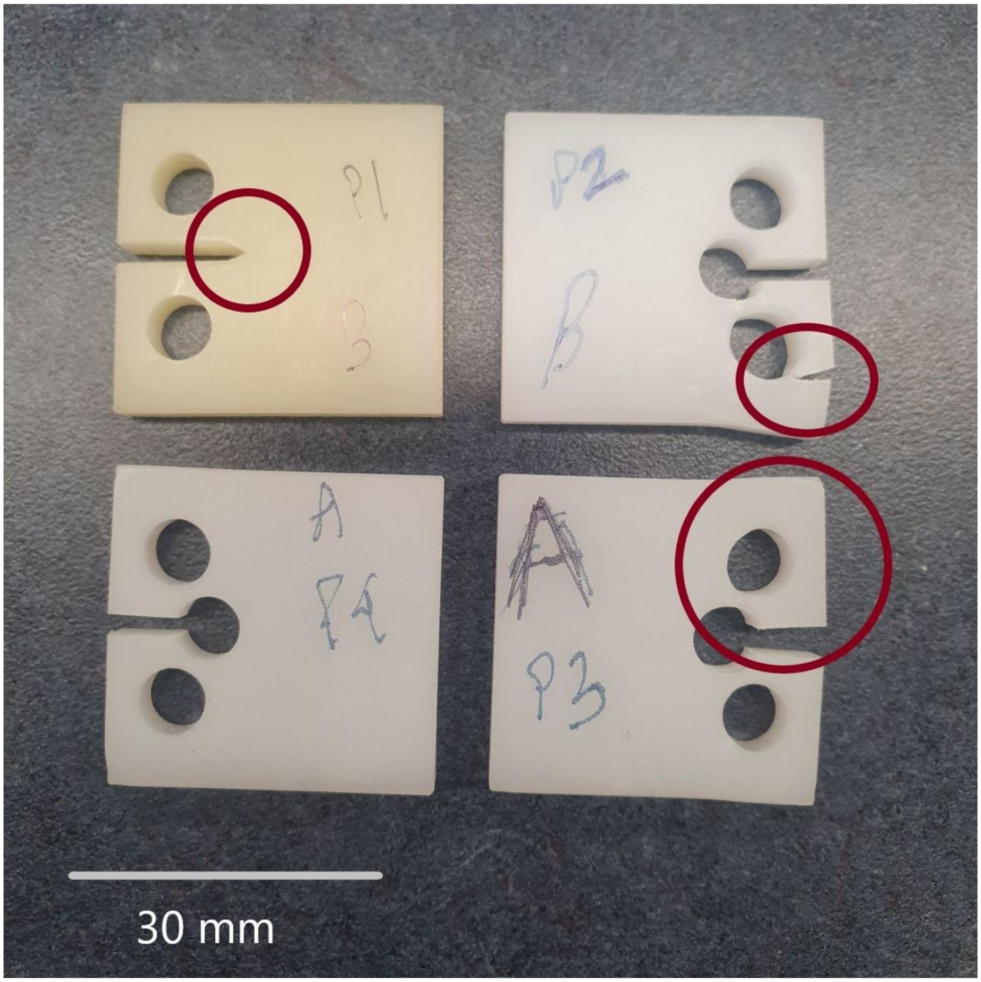


**Figure 10** Samples P1-P4 (displayed clockwise from top-left) post completion of fatigue tests.

To enhance the possibility of crack initiation and eventual fatigue failure, the next set of samples (P5-P10) were made from a block of VXLPE which is known to have a reduced fatigue resistance vis-à-vis UHMWPE (Baker, Bellare, and Pruitt 2003; Medel et al. 2007), the a/W ratio was increased to 0.35, 0.5, and 0.6, and the notches were made sharper with a notch root radius of 0.25 mm.

Figure 11 shows the samples P5-P10 after each of them failed through fatigue testing. Experiments were restarted on sample P5 at the load range of 18-180N and tested for a total of 75000 cycles and then incrementally increased through 20-200N, 22-220N, 25-250N, till a load range of 28-280N when it broke into two parts symmetrically after limited cycles (9315 cycles). Since sample P6 had a higher a/W ratio of 0.5 vis-à-vis P5 (a/W ratio 0.35), the stress intensity experienced at the crack tip (notch root in this case) would be higher. Consequently, the load was reduced prior to the next series of fatigue tests with higher a/W ratio, given the direct correlation between stress intensity experienced at the crack tip with the load range as formulated in Equation A1.3 of the ASTM standard ("ASTM E647-15e1 - Standard Test Method for Measurement of Fatigue Crack Growth Rates" 2015). Sample P6 was fatigued at 10-100N initially. However, given the inaccuracies in the load control system of the machine, the minimum load often went lower than 10N culminating in one of the pins loosening and falling out time and again. To surmount this, the loading was slightly increased to 15-150N and finally to 20-200N after which the sample failed through fatigue at a limited number of cycles (1561 cycles). Next, sample P7 with an a/W ratio of 0.6 was loaded at 20-200N and the experiment failed within moments of initiation. The fatigue cycles on P7 were recorded as 86 cycles at failure. In the three aforementioned samples P5-P7, the crack initiation was traced back to the notch root region, akin to the crack tip in a conventional C(T) sample.

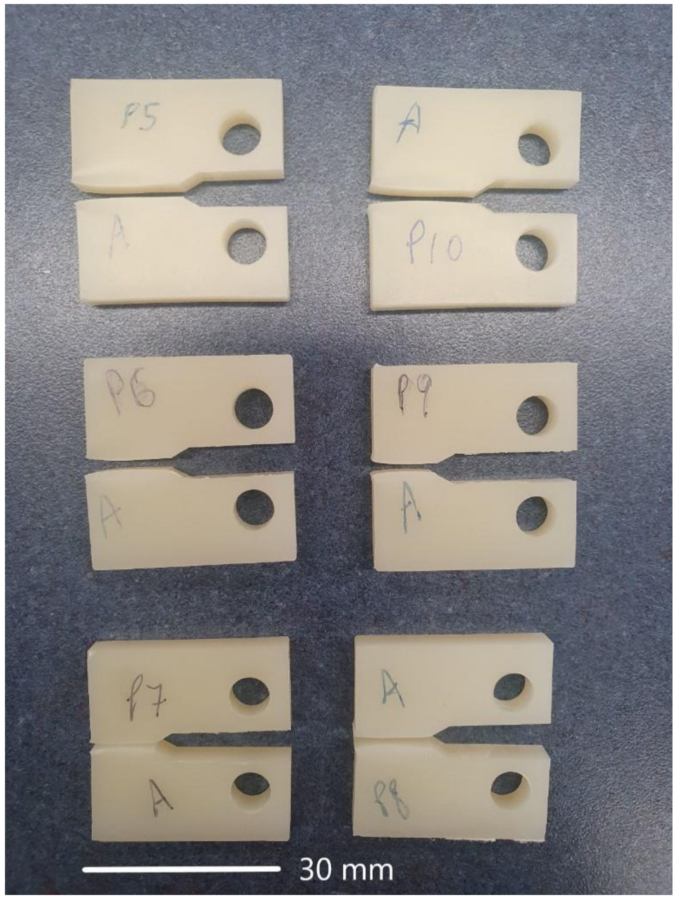


**Figure 11** Samples P5-P10 (displayed anti-clockwise from top-left) after they failed via fatigue.

To examine the damage accumulation effect of the lower loads or lack thereof, the next series of samples P8-P10 were fatigue cycled at the highest load at which their counterparts (P5-P7) failed. Sample P8 (same family as P6) was fatigue cycled at 20-200N and it failed at 3849 cycles, which marks a 146% increase in fatigue life. Sample P9 (same family as P7) was tested at 20-200N, and it broke at 71 cycles, very close to the original sample P7's 86 cycles fatigue failure value. Here, the damage accumulation concept is not applicable since the samples were tested at the same load range. Finally, for sample P10 (same family as P5), loading was initiated at 28-280N and it failed at 12539 cycles, a 34% increase from sample P5. The significant addition in the fatigue lives of samples P8 and P10 in comparison to P6 and P5 respectively, holds testament to the damage accumulation at the lower load cycles and attests to the additive effect formulated in Palmgren-Miner's rule (Palmgren 1924; Miner 1945).

**Table 4** Compilation of a/W ratio, stress intensity values, and number of cycles to fatigue failure for samples P7-P10.

| Sample | a/W ratio | ΔK (MPa√m) | $N_{failure}$ |
|---|---|---|---|
| P7 | 0.6 | 3.1915 | 86 |
| P8 | 0.5 | 2.2356 | 3849 |
| P9 | 0.6 | 3.2071 | 71 |
| P10 | 0.35 | 2.0404 | 12539 |

Given that UHMWPE is a fatigue brittle polymer, the crack initiation length couldn't be determined during fatigue experiments. The samples P7-P10 fatigued to failure catastrophically, precluding any observation of the crack's initiation or its measurement thereof. Consequently, all calculations reported herein are based solely on the a/W ratio. An increase in a/W ratio enforces a stronger stress intensity at the notch root. Table 4 compiles the ΔK values, number of cycles to failure, and a/W ratio for samples P7-P10 which are of interest in this study. Further,

Figure clearly shows how increasing stress intensity at the crack tip (increased a/W ratio) leads to a reduction in the fatigue life, as is theoretically expected and also, experimentally confirmed. The data from samples P7-P10 (fatigued at highest loads only) is plotted herein. The values of ΔK obtained in this study are higher than the threshold ΔK values obtained in another study, whereby $\Delta K_{threshold}$ = 1.08 MPa√m was obtained. Noteworthy to add here that the threshold data was collected in a radically different manner which involved running $\Delta K_{decreasing}$ tests up until the point where the crack growth rate was less than $10^{-7}$ mm/cycle. This may also be attributed to the fatigue brittle nature of UHMWPE and its sensitivity to peak stress intensity.

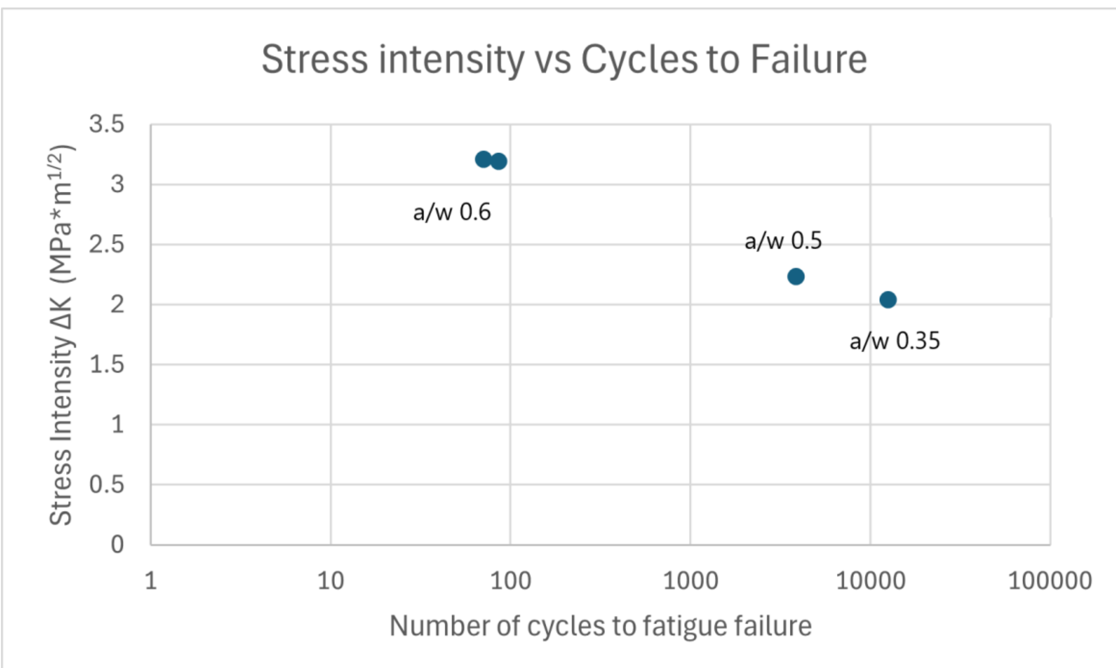


**Figure 12** Stress intensity ΔK vs Number of cycles to failure (N) for the material type VXLPE.

Going forward, the a/W ratio of 0.6 may be discarded due to the excessively high stress intensity it imparts at the notch root and the extremely low number of fatigue cycles noted.

Similarly, the a/W ratio of 0.25 should be avoided, especially for samples with higher notch root radii of 3mm as they might jeopardize the experiments by inadvertently creating undue stress concentrations in the region between the notch and pin holes. Future experiments must therefore work within the optimal window of a/W ratios spanning 0.35 to 0.5. Moreover, future parametric studies to be conducted can encompass different notch root radii including but not limited to 0.25, 1, and 3 mm, and different a/W ratios (range 0.35-0.5) as well as both sets of materials (UHMWPE and VXLPE) and decipher their individual and synergetic effects on the fatigue life. A parametric model with notch root radii, a/W ratio, and UHMWPE formulation as input parameters and fatigue life as the output parameter can be systematically developed thereafter. Efforts towards monitoring the moment of crack initiation can be undertaken by precisely syncing the frame rate of the optical camera for observing the fatigue test specimen and the frequency of the fatigue testing (5 Hz). That way, the sample would appear stationary and the exact moment a crack nucleates at or in the vicinity of the notch root, can be easily monitored. Crack initiation criteria could then be modified to $N_{initiation}$ instead of $N_{failure}$, even if the difference between the values is very marginal for a fatigue brittle polymer like UHMWPE.

### 3.6 Conclusions

This chapter summarizes some of the preliminary findings concerning the crack initiation behavior of UHMWPE with different a/W ratios, studied by fatiguing the samples to failure. The key results reaffirm the inverse relation between a/W ratio and the number of fatigue cycles to failure, which can be explained on account of the increased stress intensity experienced at the crack tip (notch root) for samples with higher a/W ratios. Additionally, the damage accumulation theory of Palmgren-Miner is evident by virtue of the significantly increased lifetime of samples from the same family (geometry, material formulation) when tested only at the highest load vis-à-vis the incremental increase in load. Future work could use multiple samples across different material formulations and aim to develop a parametric model encompassing three parameters of interest, viz. material formulation, a/W ratio, notch root radii and their relationship to the crack initiation behavior as well as fatigue life of UHMWPE.

# Chapter 4 – Characterization of the fatigue threshold behavior of UHMWPE

*This chapter has been published in the Journal of the Mechanical Behavior of Biomedical Materials (Smith, Roy, Ritchie, and Pruitt 2025)*

## 4.1 Chapter Summary (Abstract)

Ultra-high-molecular-weight-polyethylene (UHMWPE) has been the material of choice for bearings in total joint replacements (TJRs) for decades as a result of its excellent wear resistance, chemical inertness, energetic toughness, low friction, and biocompatibility. Utilization of this polymer in orthopedic devices requires oxidation, wear, and fatigue resistance. Balancing these important properties by tailoring processing techniques and modulating microstructural features has been an ongoing endeavor in the field. Research into the clinical applications of UHMWPE has primarily focused on the challenges of wear and oxidation while studies into the realm of fatigue have been more limited. Literature gaps exist in fully understanding the fatigue crack initiation near notches or propagation of small existing flaws in UHMWPE used in TJRs. In particular, the characterization of the fatigue thresholds and near-threshold fatigue behavior of orthopedic grade UHMWPE has yet to be thoroughly explored. In this work, we characterized the fatigue crack arrest threshold of clinically-relevant UHMWPE formulations. Correlations between the fatigue thresholds and bulk mechanical properties as well as microstructural properties were examined across these medical resins. The important role played by crosslinking in influencing the fatigue performance of UHMWPE is highlighted in this study. In addition, it is established that J-integral fracture toughness is the best predictor of fatigue thresholds and could possibly be used as a stand-in metric for fatigue performance if thresholds cannot be directly ascertained. Finally, this study corroborates that the true constitutive parameters best describe the mechanical behavior of UHMWPE.

## 4.2 Fatigue in UHMWPE

Ultra-high-molecular-weight-polyethylene (UHMWPE) has been the material of choice for the bearing surface of total joint replacements (TJRs) since the 1960's (Charnley, 1973). The choice of UHMWPE arises from an array of unique bio-tribo-mechanical attributes including but not limited to abrasion and wear resistance, chemical inertness, energetic toughness, low friction, and biocompatibility (Kurtz, 2009). Despite its excellent bio-tribo-mechanical performance *in-vivo*, UHMWPE in total knee arthroplasty is subjected to high-amplitude cyclic contact stresses and must endure loading for 20-30 million cycles (Sobieraj & Rimnac, 2009). Such extensive biomechanical demands can culminate in the generation of sub-micron sized wear debris, leading to osteolysis, implant loosening, and eventually, failure of the TJR. In addition to the production of wear debris, catastrophic failure of the implant due to fast fracture from fatigue damage accumulation is also a potential issue (Ansari, Gludovatz, *et al*., 2016). In order to mitigate these potential failure modes, there is an ongoing effort to develop formulations of UHMWPE that resist the troika of challenges faced in the body – wear, fatigue, and oxidation (Ansari, Ries, *et al*., 2016; Atwood *et al*., 2011). Though no one specific formulation is ideal for every patient or failure modality, modern implants are typically made of moderately crosslinked UHMWPE which has been remelted with vitamin E additives, to protect it from oxidation while moderately balancing fatigue and wear properties (Bistolfi *et al*., 2021; Bracco & Oral, 2011). Understanding the interplay between these processing techniques, corresponding microstructures, and concomitant mechanical properties is an ongoing endeavor, even though the existing body of literature about UHMWPE for TJRs is quite extensive (Ansari, Gludovatz, *et al*., 2016; Ansari, Ries, *et al*., 2016; Baker *et al*., 2000, 2003; Connelly *et al*., 1984; Furmanski & Pruitt, 2007; Gencur *et al*., 2006; Patten *et al*., 2011; Pruitt, 2005; Pruitt *et al*., 2022; Simis *et al*., 2006; Sirimamilla *et al*., 2013a; Sirimamilla & Rimnac, 2019). However, there are still literature gaps that exist in understanding the fatigue behavior around crack initiation near notches or propagation of small existing flaws in orthopedic grade UHMWPE used in modern implant designs. In particular, the characterization of the fatigue threshold and near-threshold crack growth behavior across multiple clinically-relevant formulations of UHMWPE has yet to be thoroughly explored.

In linear elastic fracture mechanics (LEFM), the fatigue threshold, $\Delta K_{\mathrm{th}}$, as a concept, refers to the stress intensity range below which cracks do not propagate under cyclic loading conditions (Davidson & Suresh, 1984; Ritchie, 1977; Schmidt & Paris, 1973). Determining the threshold experimentally requires careful methodology. The benefit of characterizing fatigue threshold or crack arrest threshold is the determination of a parameter that can be utilized in safety-critical design for orthopedic components known to have notches and elevated cyclic stresses.

In the field of fatigue of metals and alloys, the methods outlined in ASTM E647 (*Standard Test Method for Measurement of Fatigue Crack Growth Rates*, 2024) are commonly used to measure and determine $\Delta K_{\mathrm{th}}$. ASTM E647 defines $\Delta K_{\mathrm{th}}$ as the asymptotic value of $\Delta K$ on a d$a$/d$N$ vs. $\Delta K$ log-log plot at which d$a$/d$N$ approaches vanishingly small rates. The standard further suggests using an operational definition of $\Delta K_{\mathrm{th}}$ as the $\Delta K$ at which d$a$/d$N$ = $10^{-7}$ mm/cycle. To experimentally determine this ASTM-defined $\Delta K_{\mathrm{th}}$, a load-shedding approach is utilized. This is accomplished by cyclically loading a sample starting at a $\Delta K$ value above $\Delta K_{\mathrm{th}}$ - somewhere near the start of the Paris regime as determined from literature and then decreasing the load in a controlled manner to mitigate fluctuations in stress intensity factor and concomitant anomalous fluctuations in d$a$/d$N$ (Saxena *et al*., 1978).

Fatigue characterization of polymers is generally more complicated than that of conventional metals or alloys. Polymers are viscoelastic and susceptible to hysteretic heating, typically limiting the test frequencies to 5 Hz or less. Specimen geometries can complicate the matter as overtly thick specimens can result in internal heating that can alter microstructure and fatigue behavior (Ansari, Ries, *et al*., 2016; Hertzberg *et al*., 1979; Pruitt *et al*., 2022). Much of the UHMWPE fatigue data reported in the literature provides only Paris regime behavior at 5 Hz or less in thermally controlled environments. There remains a paucity of data or literature that focuses on classical fatigue threshold values for UHMWPE. Instead, the orthopedic community has utilized a much less conservative parameter, coined $\Delta K_{\mathrm{Inception}}$ (Baker *et al*., 2000, 2003; Gencur *et al*., 2006). This metric is derived empirically from the onset of the Paris regime and is defined as the $\Delta K$ at which d$a$/d$N$ = $10^{-6}$ mm/cycle (Baker *et al*., 2000, 2003; Pruitt, 2005). One key difference between $\Delta K_{\mathrm{th}}$ as defined previously and $\Delta K_{\mathrm{Inception}}$ is the loading regiment used to find these parameters. $\Delta K_{\mathrm{Inception}}$ is found using only constant or increasing loads, resulting in an increasing $\Delta K$ due to crack growth throughout the test, limiting the scope of the metric. A more recent study that investigated fatigue crack initiation in UHMWPE (Sirimamilla & Rimnac, 2019) reported the number of cycles to failure for various waveforms and a maximum load of 800 N instead of $\Delta K_{\text{Inception}}$ or $\Delta K_{\text{th}}$. Our research endeavor intends to expand these concepts by determining $\Delta K_{\text{th}}$ as defined by ASTM E647 for seven different clinically relevant formulations of UHMWPE. To the authors' knowledge, this is the first study to characterize the fatigue threshold behavior of UHMWPE.

It is essential to enumerate why studying fatigue thresholds and near-threshold crack growth rates is paramount for the orthopedic applications of UHMWPE. All TJRs inherently have stress concentrations or notches built into their locking mechanisms and clinical functionality of the device (Ansari, Gludovatz, *et al*., 2016; Ansari, Ries, *et al*., 2016; Kurtz, 2009; Sirimamilla & Rimnac, 2019). These regions of heightened stress states are prone to crack initiation and crack growth (Furmanski, Anderson, *et al*., 2009; Furmanski & Pruitt, 2018; Pruitt & Furmanski, 2009). The majority of a crack's lifetime is spent in initiation rather than in propagation in UHMWPE because the material is fundamentally fatigue brittle (Barsom & Rolfe, 1999; Davidson & Suresh, 1984; Furmanski & Pruitt, 2007; Pruitt, 2005). Understanding a crack's initiation behavior or stress state required for initial growth of an existing flaw is clinically important for TJR, yet the predominant characterization of UHMWPE is based on Paris regime behavior. The Paris regime is important for understanding fatigue but only captures crack propagation behavior at the mid-range of growth rates, typically between ~$10^{-5}$ to $10^{-2}$ mm/cycle (Barsom & Rolfe, 1999; Hertzberg *et al*., 2012; Kurtz, 2009; Pruitt *et al*., 2022). Fatigue thresholds, conversely, are a more relevant fatigue parameter for designing against catastrophic failures and in safety-critical applications such as TJRs.

The fatigue threshold is pertinent as it reveals the minimum stress intensity range at which a flaw will commence propagation before it traverses through the Paris regime and culminates in fast fracture. However, little is known regarding the UHMWPE threshold even though other aspects of its fatigue properties are well-researched. Fatigue threshold values have never been measured directly for the UHMWPE resins utilized in TJRs. One reason for the paucity of this data may be the time investment needed for the load-shedding methodology (Nibur & Somerday, 2025).

The purpose of this study is to determine the crack arrest threshold and fatigue crack propagation behavior across seven clinically-relevant formulations of UHMWPE. This study also examines relationships between the fatigue threshold and known mechanical and microstructural properties for these clinically-relevant formulations. To the authors' knowledge, this is the first study to characterize the fatigue threshold of UHMWPE using a load-shedding method.

### 4.3 Methods and Materials

Seven different clinically relevant formulations of ultra-high molecular weight polyethylene (UHMWPE) were analyzed in this study (comprehensively tabulated in Table X). Specifically, two medical grade resins, GUR 1020 and GUR 1050, with varying amounts of vitamin E (VE) and crosslinking were examined. All resins were manufactured following industry specifications. The 1050 75 kGy resin was ram extruded and the balance of the resins were compression molded. For the VE samples, the antioxidant was blended into the GUR 1020 base resin before consolidation at 0.1 weight%. Two levels of crosslinking in 1020 (0 kGy and 35 kGy), three levels of crosslinking in 1020 VE (0 kGy, 100 kGy, and 125 kGy), and two levels of crosslinking in 1050 (0 kGy and 75 kGy) were included in the scope of this investigation. All sample groups were sourced from Orthoplastics (Lancashire, UK) except 1050 75 kGy which was sourced from Quadrant EPP (Fort Wayne, IN). At least 3 samples for each group were analyzed for statistical relevance. These clinically-relevant UHMWPE formulations were sourced from the same base materials used in our previously published studies investigating microstructure as well as bulk mechanical properties and fracture toughness (Malito *et al*., 2018, 2019). A summary of relevant properties is provided in Table 5.

Table 5: Properties of the UHMWPE resins utilized in the fatigue threshold study (Malito *et al*., 2018, 2019).

| Sample Group Name | Amount of Crosslinking radiation (kGy) | wt.% VE (%) | Percent Crystallinity (%) | Lamellar Thickness (nm) | Elastic Modulus (MPa) | Ultimate True Tensile Strength $\sigma_{UTS\ true}$ (MPa) | J-Integral Fracture Toughness $_{Ic\ true}$ (kJ/m$^2$) | Plane-strain Mode I Fracture Toughness $_{JIc}$ (MPA$\sqrt{m}$) |
|---|---|---|---|---|---|---|---|---|
| 1020 | 0 | 0 | 57.7 | 26.3 | 799.5 ± 26.2 | 188.2 ± 17 | 40.6 | 6.41 |
| 1020 35 kGy | 35 | 0 | 57.8 | 26.1 | 758 ±39.4 | 184.3 ±16.1 | N/A | N/A |
| 1020 VE | 0 | 0.1 | 60.0 | 29.3 | 921.2 ±13.6 | 229.1 ± 9.7 | 32.5 | 7.07 |
| 1020 VE 100 kGy | 100 | 0.1 | 60.7 | 27.0 | 1008.5 ± 36.6 | 146.4 ± 13.6 | 19.7 | 5.03 |
| 1020 VE 125 kGy | 125 | 0.1 | 60.8 | 28.1 | 865.4 ± 56.3 | 158.8± 9.7 | 19.5 | 4.63 |
| 1050 | 0 | 0 | 55.8 | 28.0 | 810.6 ± 26.2 | 202.8 ± 29.9 | 36.1 | 6.42 |
| 1050 75 kGy | 75 | 0 | 55.8 | 27.7 | 762.3 ± 32.0 | 127.9 ± 12.8 | 20.2 | 4.60 |

Compact tension (C(T)) specimens were machined from stock materials with dimensions adhering to ASTM E647-15 (*Standard Test Method for Measurement of Fatigue Crack Growth Rates*, 2024). It is important to state here that while ASTM E647 prescribes a set of dimensions and dimensional ratios and proportions for the specimens used for fatigue testing, the standard was originally developed for ductile metals or alloys. An upgrade to ASTM E647 standard is needed for full relevance to the fatigue testing of polymeric materials. C(T) samples had a width ($W$) of 25 mm, a thickness ($B$) of 5 mm, and a length ($L$) of 31.8 mm (Figure 13). To ensure a sharp notch, pre-cracking was performed with a clean razor blade to achieve an initial crack length ($a_0$) of 7 - 8 mm.

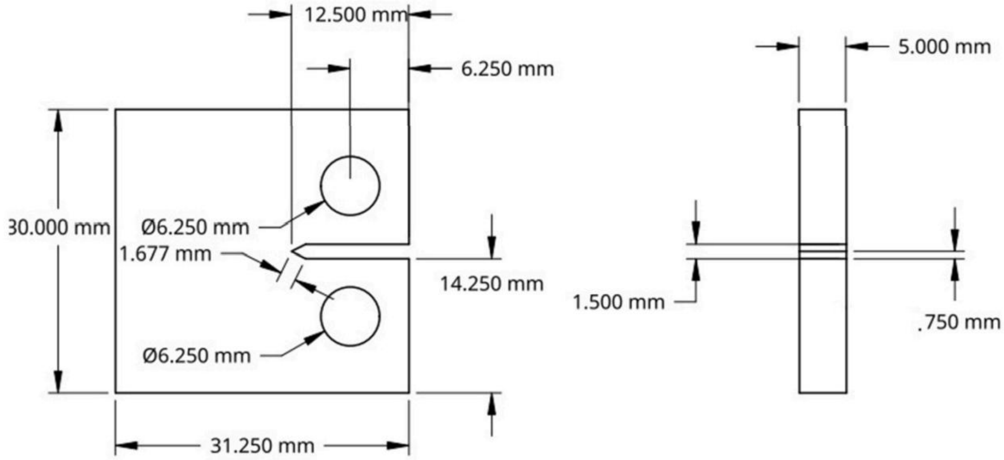


**Figure 13**: Dimensions of a typical C(T) sample used for the fatigue threshold study based on ASTM E647. Dimensions shown in mm.

Tension-tension loading-based fatigue tests were conducted on an electro-servo-hydraulic MTS Elastomer Test System Model 831 machine (Eden Prairie, MN). Crack propagation rates (d*a*/d*N*) were measured using the aforementioned compact tension specimens. Crack measurements were taken by pausing the load cycle at the midpoint load and measuring the crack length using an Olympus micromechanical stage (Tokyo, Japan) and a corresponding image from a microscope (with a resolution of 0.1 $\mu$m). Crack propagation rates (d*a*/d*N*) were then calculated using a secant method outlined in ASTM E647 and reported in units of mm/cycle. The stress-intensity range ($\Delta K$) was calculated using the standard long crack in C(T) specimens, as formulated in the ASTM E647 standard:

$$\Delta K = \frac{\Delta P}{B\sqrt{W}} f(\alpha), \tag{1}$$

where $\Delta P$ is the maximum applied load minus the minimum applied load, $B$ is the sample thickness, $W$ is the sample width, $a$ is the crack length, and $\alpha = \frac{a}{W}$ is the ratio of crack length to width. $f(\alpha)$ is formulated as follows:

$$f(\alpha) = \frac{(2+\alpha)}{(1-\alpha)^{1.5}}(0.866 - 4.64\alpha - 13.32\alpha^2 - 14.72\alpha^3 - 5.6\alpha^4) \ . \tag{2}$$

Fatigue crack propagation tests were performed to determine the fatigue thresholds for the aforementioned UHMWPE formulations using $\Delta K$ decreasing tests while the subsequent near-threshold growth rates and higher growth rates were determined under increasing $\Delta K$ tests (Barsom & Rolfe, 1999; Hertzberg *et al.*, 2012). The $\Delta K$ increasing tests were load-controlled with a frequency of 5 Hz and a sinusoidal waveform. All tests were performed at room temperature with a fan system to avoid hysteretic heating (Sobieraj & Rimnac, 2009). A load ratio of $R$ = 0.1 (ratio of minimum to maximum load) was maintained throughout testing, and the load applied was increased when necessary to ensure $\Delta K$ concomitantly increased.
For the $\Delta K$ decreasing tests, a stepped force-shedding approach was utilized (Saxena *et al.*,

1978; *Standard Test Method for Measurement of Fatigue Crack Growth Rates*, 2024). The initial load began well above the implied stress intensity range for crack arrest from the $\Delta K$ increasing tests and was then decreased at a rate consistent with ASTM E647 in order to limit abnormal data from reductions in stress-intensity factor. To do this, the normalized $K$-gradient $c$ was kept above -0.08 mm$^{-1}$ according to:

$$c = \frac{1}{K}\left(\frac{dK}{da}\right) > -0.08 \text{ mm}^{-1} \tag{3}$$

Practically, this means that each $\Delta K$ after the initial $\Delta K_0$ was determined by the following exponential decay equation:

$$\Delta K_n = \Delta K_0 exp[C(a_{n-1} - a_o)] \tag{4}$$

Here $\Delta K_0$ is the initial $\Delta K$ selected to be far above the threshold, $a_0$ is the initial crack length, $a_{n-1}$ is the crack length measured, the normalized $K$-gradient $c$ = -0.08, and $n$ is an index beginning at 2 (2,3,4, etc.). Each $\Delta K$ was calculated using the crack length preceding it, so the first two data points in each test were excluded. The crack arrest threshold ($\Delta K_{th}$) was defined as the $\Delta K$ at which the growth rate d$a$/d$N$ was less than $10^{-7}$ mm/cycle for at least 3 steps down the force-shedding regimen. After reaching the threshold, the sample would then be subject to the $\Delta K$ increasing test to ensure the d$a$/d$N$ rates matched both going up and down for a given $\Delta K$. Consequently, d$a$/d$N$ vs. $\Delta K$ was traced on a log-log plot.

After experimentally ascertaining the d$a$/d$N$ and calculating the $\Delta K$ values, the Paris regime constants $C$ and $m$ were calculated in the range of d$a$/d$N$ from $10^{-6}$ to $10^{-5}$ as outlined in ASTM E647. By fitting a line using the least squares method to the log-log plot of d$a$/d$N$ vs. $\Delta K$, one can determine the values of $C$ and $m$ using the following equation:

$$log\left(\frac{da}{dN}\right) = mlog(\Delta K) + log(C)\,. \tag{5}$$

In addition, relationships between the threshold ($\Delta K_{th}$), $J$-integral fracture toughness ($J_{Ic\ true}$), plane-strain mode I fracture toughness ($K_{JIc}$), elastic modulus ($E$), and ultimate true tensile stress ($\sigma_{UTS\ true}$), as well as percent crystallinity and lamellar thickness, were analyzed using a non-parametric Spearman rank correlation coefficient (Atwood *et al*., 2011; Malito *et al*., 2018). Spearman rank correlation is an appropriate test to run because we expect monotonic relationships between the variables explored in this study. Average values were used for the correlations. $J_{Ic\ true}$, $K_{JIc}$ as well as the bulk mechanical and microstructural properties for the specific material groups in this work were experimentally measured in previous studies published from our lab (Malito *et al*., 2018, 2019).

## 4.4 Results

The d$a$/d$N$ vs. $\Delta K$ curves for the seven clinical formulations of UHMWPE are comprehensively compiled and illustrated in Figure 14. On this logarithmic plot of crack propagation rate (mm/cycle) as a function of stress intensity range (MPa√m), we illustrate both near-threshold and Paris regime fatigue resistance of the UHMWPE resins spanning a range of crosslinking and antioxidant dose. Inspection of these plots indicate that the highly crosslinked materials have lower crack arrest thresholds and a reduced fatigue crack propagation resistance than the formulations with less crosslinking. The average crack-arrest fatigue thresholds ($\Delta K_{th}$) and the regime constants (coefficient and exponent) are reported in Table 6.

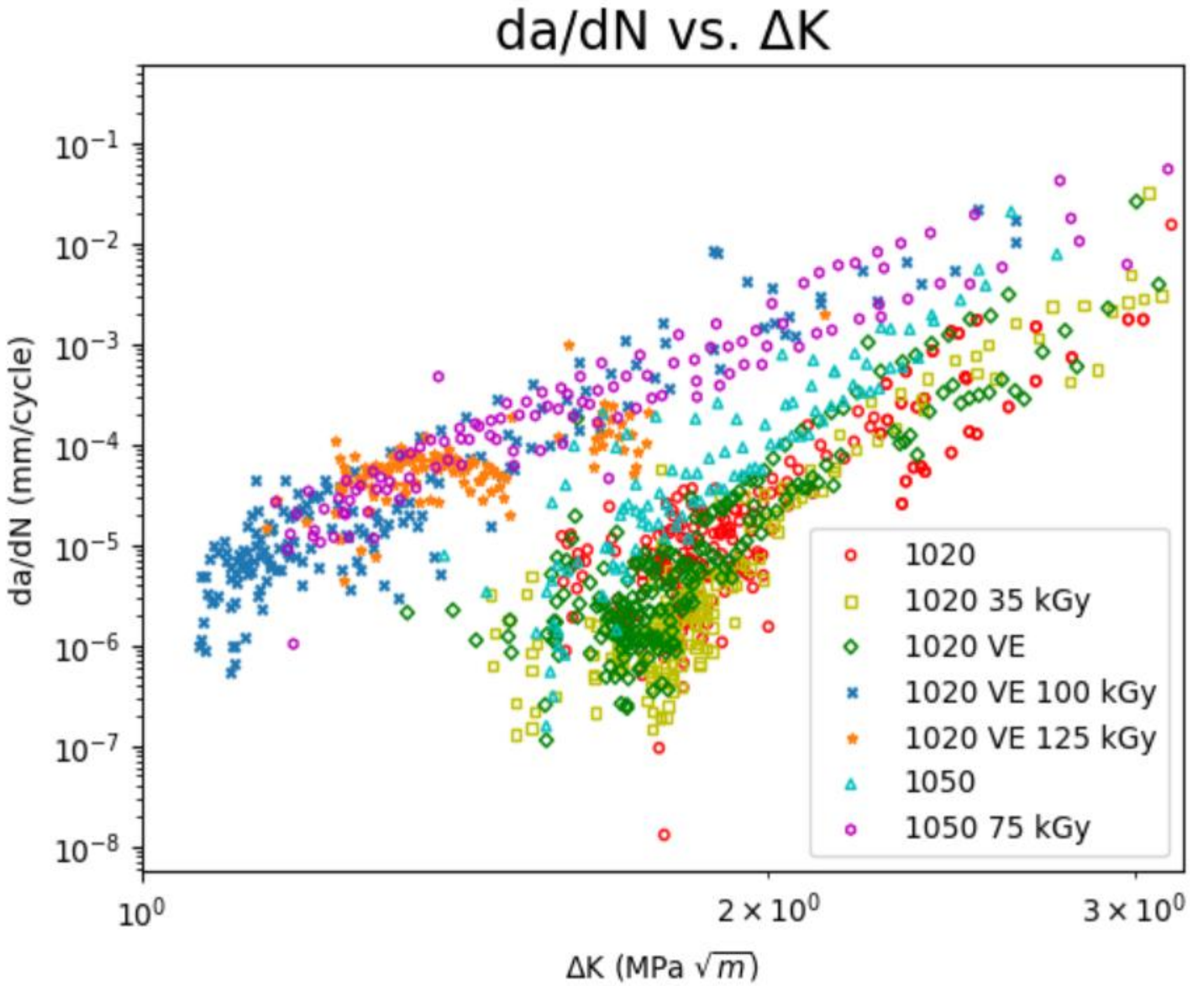


**Figure 14**: Crack propagation (d$a$/d$N$) as a function of stress intensity range ($\Delta K$) plots for the clinical formulations of UHMWPE tested in this study.

**Table 6:** Paris regime coefficients ($C, m$) and fatigue thresholds ($\Delta K_{th}$) for the clinical formulations of UHMWPE tested in the fatigue threshold study.

| UHMWPE Group | Paris regime constants | | $\Delta K_{th}$ (MPa$\sqrt{m}$) |
|---|---|---|---|
| | Exponent ($m$) | Coefficient ($C$) ($\frac{mm}{cycle}$/(MPa$\sqrt{m}$)$^m$) | |
| 1020 | 11.77 | 5.5 x $10^{-9}$ | 1.76 $\pm$ 0.16 |
| 1020 35 kGy | 14.63 | 3.9 x $10^{-10}$ | 1.66 $\pm$ 0.15 |
| 1020 VE | 13.55 | 1.7 x $10^{-9}$ | 1.61 $\pm$ 0.05 |
| 1020 VE 100 kGy | 9.84 | 1.8 x $10^{-6}$ | 1.15 $\pm$ 0.12 |
| 1020 VE 125 kGy | 4.82 | 1.1 x $10^{-5}$ | 1.17 $\pm$ 0.07 |
| 1050 | 13.74 | 8.8 x $10^{-9}$ | 1.58 $\pm$ 0.04 |
| 1050 75 kGy | 6.75 | 8.6 x $10^{-6}$ | 1.22 $\pm$ 0.13 |

Table 7 displays the Spearman rank correlation coefficients with their respective p-values between crack arrest threshold ($\Delta K_{th}$) and mechanical properties as well as crystallinity and lamellar thickness. Our findings indicate that there is no statistically significant correlation between $\Delta K_{th}$ and the microstructural properties of the UHMWPE formulations. However, the findings show a statistically significant ($p < 0.05$) correlation coefficient between $\Delta K_{th}$ and $J$-integral fracture toughness ($J_{Ic\ true}$). If $p < 0.1$ is considered to be statistically significant, then correlations also exist between $\Delta K_{th}$ and ultimate true tensile strength ($\sigma_{UTS\ true}$) and plane-strain mode I fracture toughness ($K_{JIc}$).

**Table 7:** Spearman rank correlation coefficients between crack arrest thresholds and microstructural as well as mechanical properties (Malito *et al.*, 2018, 2019).

| Crack Arrest Threshold<br><br>p-value significance | Percent Crystallinity (%) | Lamellar Thickness (nm) | Elastic Modulus $E$ (MPa) | True Ultimate Tensile Strength $\sigma_{UTS\ true}$ (MPa) | J-Integral Fracture Toughness $J_{Ic\ true}$ (kJ/m$^2$) | Plane-Strain Mode I Fracture Toughness $K_{JIc}$ (MPa$\sqrt{m}$) |
|---|---|---|---|---|---|---|
| $\Delta K_{th}$ (MPa$\sqrt{}$m) | -0.198 | -0.0714 | 0.00 | 0.714 | 0.829 | 0.771 |
| **p-value** | 0.67 | 0.89 | 0.88 | 0.052 | 0.042 | 0.072 |
| **Significant** (p<0.05, p<0.1) | No | No | No | Yes, $p < 0.1$ | Yes, $p < 0.05$ | Yes, $p < 0.1$ |

### 4.5 Discussion

This study offers a number of technical findings, some of which follow the well-established and classical understanding of UHMWPE fatigue behavior while others differ from the "norms" of the field. This work is the first to report experimental $\Delta K_{th}$ values and to examine correlations across a volley of microstructural and mechanical properties. In terms of expected results, our fitted values for $C$ and $m$ in the Paris regime are consistent with those reported previously for similar formulations of UHMWPE in the literature (Baker *et al.*, 2003; Furmanski & Rimnac, 2011; Gencur *et al.*, 2006). Though the fatigue thresholds were not examined in prior studies, it is reassuring to note that the Paris regime behavior results are in consonance across the literature.

Another encouraging result is that crosslinking is the defining factor that influences the fatigue performance of the formulations considered in this study. Four of the seven sample groups (viz. 1020, 1020 VE, 1020 35 kGy, and 1050) have $\Delta K_{th}$ values that are statistically the same, *i.e.*, fall within the standard error margin of each other. The sample groups that have significantly different $\Delta K_{th}$ from these (namely, 1050 75 kGy, 1020 VE 100 kGy, and 1020 125 kGy) have undergone higher doses of crosslinking. Similar trends in $C$ and $m$ values are observed as well, with the former UHMWPE groups with little-to-no crosslinking having similar orders of magnitude for $C$ ($10^{-9}$ to $10^{-10}$) *vis-a-vis* $C$ values between $10^{-6}$ to $10^{-5}$ for the highly crosslinked groups (Furmanski & Rimnac, 2011). These also exhibited higher $m$ values than the latter groups as was observed in another study (Baker *et al.*, 2003). Crosslinking significantly reduces fatigue crack propagation resistance which is congruous with the trends reported in the literature (Ansari, Ries, *et al.*, 2016; Atwood *et al.*, 2011; Baker *et al.*, 2003; Cole *et al.*, 2002; Gencur *et al.*, 2006; Medel *et al.*, 2007; Sobieraj & Rimnac, 2009). Conclusively, crosslinking, which is typically undertaken to improve the wear resistance of UHMWPE in orthopedic medical devices, comes at the expense of its fatigue resistance.

Interestingly, no correlation was found to exist between elastic modulus ($E$) and $\Delta K_{th}$, even though $E$ has been successfully related to fatigue crack propagation in the past (Hertzberg *et al.*, 1970, 1979). Specifically, in ductile materials where a fatigue crack propagates by crack-tip blunting followed by resharpening over the loading cycle, a high elastic modulus tends to reduce the crack-opening displacement which should then lower the crack extension each cycle. Since different deformation mechanisms govern fatigue crack propagation *vs.* fatigue crack initiation/arrest, it is possible that parameters correlating with one have little to no correlation with the other, thus explaining why $E$ did not correlate with $\Delta K_{th}$ in the present study. Previous work has shown that fatigue crack growth in UHMWPE follows a fatigue-brittle mechanism and as such more tightly correlates with fracture toughness rather than modulus (Furmanski, Rimnac, *et al*., 2009; Pruitt & Furmanski, 2009).

On a similar note, there was also no correlation between $\Delta K_{th}$ and percent crystallinity. Previous studies have shown that higher crystallinity should result in higher resistance for both fatigue crack initiation and propagation due to crystalline regions impeding crack growth by means of crack deflection (Ansari, Ries, *et al*., 2016; Atwood *et al*., 2011; Baker *et al*., 2003; Niinomi *et al*., 2001; Oral *et al*., 2006). This trend was not observed in the present study. The percent crystallinity values for all seven sample groups in our study were only marginally different, ranging from 55.8% to 60.8%. This narrow range of crystallinities is likely insufficient to directly influence the fatigue properties.

The most important result derived from this study is that $J$-integral fracture toughness ($J_{\mathrm{Ic\ true}}$) is the best predictor of $\Delta K_{th}$, and could possibly be used as a stand-in metric for fatigue crack arrest/initiation if $\Delta K_{th}$ cannot be ascertained. This is in agreement with findings from another study where $\Delta K_{inception}$ was found to correlate with $J_{\mathrm{Ic\ true}}$ (Furmanski & Pruitt, 2007, 2018; Sirimamilla *et al*., 2013a). Other relevant predictors of $\Delta K_{th}$ are ultimate true tensile strength ($\sigma_{\mathrm{UTS\ true}}$) and the plane-strain mode I fracture toughness ($K_{\mathrm{JIc}}$), though $J$-integral remains the most significant with a p-value less than 0.05. Recently, arguments have been made to use true stress instead of engineering stress when analyzing the behavior of UHMWPE (Malito *et al*., 2019), and our results strongly support this argument of using true constitutive behavior. These findings also support the idea that UHMWPE fatigue behavior is best modelled by the viscoelastic fracture theory (Williams, 1977), an idea which is gradually gaining traction in the UHMWPE community (Furmanski & Pruitt, 2018; Sirimamilla *et al*., 2013b).

### 4.6 Conclusions

In summary, this is the first study to fully characterize the fatigue crack (arrest) threshold behavior and to correlate measured ΔKth threshold values to bulk mechanical and microstructural properties across a wide range of clinically-relevant UHMWPE formulations. Paris regime parameters for the mid-range of growth rates (~10-5 to 10-2 mm/cycle) were also experimentally determined and were found to be consistent with the literature. There are also two major takeaways from our findings. First, crosslinking, which is typically undertaken to improve the wear resistance of UHMWPE for use in total joint replacements, comes at the expense of fatigue resistance. Our study demonstrates that increased crosslinking decreases the fatigue threshold and reduces fatigue crack propagation resistance in UHMWPE. Secondly, the best predictor of fatigue performance for this class of materials is the J-integral fracture toughness. Other less statistically significant but still relevant predictors of fatigue threshold include the ultimate true tensile strength and plane-strain mode I fracture toughness. While the fatigue threshold, J-integral fracture toughness, ultimate true tensile strength, and plane-strain mode I fracture toughness are experimentally more challenging to determine than many engineering parameters, the authors contend that it is worth characterizing the true behavior of

UHMWPE to make better design decisions in the orthopedic medical device realm and support the idea that true constitutive behavior is ultimately the best descriptor for UHMWPE.

### 4.7 Acknowledgement and Funding Statement for This Chapter

The authors would like to thank the following people for assistance with the project: Samantha Kwan, Jon Ell, Varun Rao, Alex Sangster, Hannah Lim, Taniel Keosseian, Qin Yu, and Punit Kumar. This work was partially supported by the endowment from the Lawrence Talbot Endowed Professorship (LAP), and the SURF-SMART program 2021 as well as the summer fellowship during 2024 from the Berkeley Graduate Division (BBS) at the University of California, Berkeley. The fatigue testing facilities were supported by the Damage-Tolerance in Structural Materials (KC-13) at the Lawrence Berkeley National Laboratory, funded under contract DE-AC02-CH11231 by the U.S. Department of Energy, Office of Science, Office of Basic Energy Sciences, Materials Sciences and Engineering Division (ROR).

# Chapter 5 – Conclusions and Future Directions

Osteoarthritis remains a disease that affects about 10 percent of people at some point in their lives. To alleviate severe cases of osteoarthritis, total joint replacement (TJR) of the affected area (typically hip, knee or shoulder) is employed. TJRs primarily use a polymer bearing with a ceramic or metallic counter-bearing as articulating components. The polymer of choice for the bearing is ultra-high molecular weight polyethylene (UHMWPE), which was chosen for a multitude of reasons such as its energetic toughness, mechanical strength, biocompatibility, and more. While this legacy material has been used for over 50 years for TJRs, there are still literature gaps in understanding its fatigue properties, especially in understanding crack initiation and fatigue threshold. This thesis provides research that fills these gaps and provides a pathway for understanding the crack inception behavior of a highly medically relevant polymer.

This dissertation reviews the complex topic of fatigue of polymers (Chapter 2). The two primary theoretical models that characterize fatigue life, the total-life and the defect-tolerant philosophies, are thoroughly discussed. The key distinction is that the first approach assumes the material starts without defects and that much of the fatigue life is spent forming a crack, whereas the second assumes materials contain initial flaws/stress concentrators and that stable crack growth comprises the majority of the component's fatigue life before final fracture. Both approaches rely on assumptions that may not hold for the entire service life of a structural part, so employing both approaches is important to fully characterize the fatigue behavior of the material. This is why the studies in Chapters 3 and 4 use the two different philosophies.

In addition to the discussion of the different philosophies, factors that dramatically influence fatigue life and fatigue micro-mechanisms in polymers are explored. These include environmental and testing variables such as frequency, strain rate, waveform, temperature, and ambient environment. Other microstructural and molecular affecting fatigue performance are also discussed, such as molecular weight, crystallinity, and crosslinking density. The information about factors that influence fatigue performance guided the experimental design of Chapters 3 and 4. Frequencies were kept low to limit hysteretic heating, and a sine waveform was used. The molecular/microstructural variables were the focus of the threshold study in Chapter 4, the main differences between sample groups. Chapter 2 acts as a key resource for researchers since it encompasses works from long ago through today, providing basically everything one would need to know as an introduction to fatigue in polymers. It also gives the required context needed to understand the experiments presented in Chapters 3 and 4.

Chapter 3 then reports initial findings for a study in crack initiation behavior in UHMWPE. Since the overwhelming majority of studies in the literature are about crack propagation, the goal here was to investigate crack initiation from geometries like notches that are unavoidable in TJR design. This was done by cycling C(T) samples of two different medical grade UHMWPE formulations until failure, using the total-life philosophy. Other factors varied were a/W ratios and notch geometry. The results indicate an inverse relationship between a/W ratio and number of cycles to fatigue failure. This happens because an increased stress intensity occurs at the crack tip when a/W is increased, thus reducing the number of cycles to initiation and failure. Another key finding is that the Palmgren-Miner rule was proven true because specimens that did not have their loads incrementally increased had much higher fatigue lifetimes than those that did have incrementally increased loads, indicating damage accrued during different the different loadings. Further studies are absolutely necessary to confirm these initial findings as statistically relevant; however, it may be possible to develop a model that can predict crack initiation behavior and cycles to failure as a function of notch root radii, a/W ratio, and medical formulation with future work.

Finally, Chapter 4 relays a completed, published study about fatigue threshold behavior in 6 medical formulations of UHMWPE. Though fatigue threshold studies performed by the load-shedding technique are somewhat common when studying metals, this is the first record of the technique being applied to UHMWPE. There are three main findings of this study. The first is that crosslinking is the factor that influences fatigue properties more than the other variables explored in this study. Though crosslinking is necessary to reduce wear in the component, increasing crosslinking comes at the cost of fatigue resistance. The second main finding is that that J-integral fracture toughness is the best predictor of fatigue thresholds and could possibly be used as a stand-in metric for fatigue performance if thresholds cannot be directly ascertained. Fatigue threshold tests can take multiple days under constant supervision to get results for a single sample because cycling must be kept under 5 Hz to ensure the polymer doesn't heat up. It makes sense that no one has tried to do fatigue threshold tests in UHMWPE until now because it's so experimentally taxing. Using J-integral fracture toughness as a stand-in for fatigue threshold could help inform design decisions without the designer needing to run the incredibly long threshold tests. The third major finding is that true constitutive parameters best describe the mechanical behavior of UHMWPE. Though more experimentally challenging to determine, it is critical for designs to be based on parameters that correctly capture the behavior of the materials used. To build from the results of Chapter 4, future studies could repeat the experiments in an environment that more closely resembles the body, such as at body temperature and/or in a bovine serum or saline solution.

In sum, this dissertation thoroughly explores the landscape of fatigue in medical formulations of UHMWPE by providing a general literature review of fatigue in polymers and the findings of two experiments about lesser-studied aspects of fatigue: initiation and threshold. This work has broad implications to the field of orthopedic biomaterials. The published findings from this work add value to the field of medical polymers as well as the realm of polymers for other load-bearing applications.

# REFERENCES


5 Ways to Manage Arthritis | CDC. (2023, June 13). https://www.cdc.gov/arthritis/basics/management.htm

Ahmad, Z.B., Ashby, M.F., Beaumont, P.W.R., 1986. The contribution of particle-stretching to the fracture toughness of rubber modified polymers. Scripta Metallurgica 20(6), 843–848.

Amjadi, M., Fatemi, A., 2020. Creep and fatigue behaviors of High-Density Polyethylene (HDPE): Effects of temperature, mean stress, frequency, and processing technique. International Journal of Fatigue 141, 105871.

Anderson, T.L., 1995. Fracture Mechanics: Fundamentals and Applications, 2nd Edition. Ann Arbor, MI: CRC Press.

Andrews, E.H., 1969. Fatigue in polymers. In: Brown, W. (Ed.), Testing of Polymers, vol. 4. New York, NY: Wiley, pp. 237–296.

Ansari, F., 2015. The Interplay of Design and Materials in Orthopedics: Evaluating the Impact of Notch Geometry on Fatigue Failure of UHMWPE Joint Replacements. In: Ph.D. Thesis, UC Berkeley.

Ansari, F., Gludovatz, B., Kozak, A., Ritchie, R. O., Pruitt, L. A., 2016. Notch fatigue of ultrahigh molecular weight polyethylene (UHMWPE) used in total joint replacements. Journal of the Mechanical Behavior of Biomedical Materials, 60, 267–279.

Ansari, F., Ries, M., Pruitt, L., 2016. Effect of processing, sterilization and crosslinking on UHMWPE fatigue fracture and fatigue wear mechanisms in joint arthroplasty. Journal of the Mechanical Behavior of Biomedical Materials 53, 329–340.

Arad, S., Radon, J.C., Culver, L.E., 1971. Fatigue crack propagation in polymethylmethacrylate. Journal of Mechanical Engineering Science 13, 75–81.

Argon, A.S., 1989. The fundamental rate determining process in creep fracture. In: Samala, K., Ravi-Chander, K., Taplin, D.M.R., Rama Rao, P. (Eds.), Proceedings of 7th International Conference on Advances in Fracture Research. New York, NY: Pergamon Press, pp. 3647–3659.

Argon, A.S., Cohen, R.E., 1990. Crazing and toughness of block copolymers and blends. In: Kausch, H.H. (Ed.), Advances in Polymer Science, vol. 91/92. Berlin: Springer, pp. 300–351.
ASTM E647-15e1—Standard Test Method for Measurement of Fatigue Crack Growth Rates. (2015). iTeh Standards.

Atwood, S. A., Van Citters, D. W., Patten, E. W., Furmanski, J., Ries, M. D., Pruitt, L. A., 2011. Tradeoffs amongst fatigue, wear, and oxidation resistance of cross-linked ultra-high molecular weight polyethylene. Journal of the Mechanical Behavior of Biomedical Materials, 4(7), 1033–1045.

Awaja, F., Zhang, S., Tripathi, M., Nikiforov, A., Pugno, N., 2017. Cracks, microcracks and fracture in polymer structures: Formation, detection, autonomic repair. Progress in Materials Science 83, 536–573.

Azimi, H.R., Pearson, R.A., Hertzberg, R.W., 1996. Fatigue of rubber-modified epoxies: Effect of particle size and volume fraction. Journal of Materials Science 31, 3777–3789.

Baker, D. A., Hastings, R. S., Pruitt, L., 1999. Study of fatigue resistance of chemical and radiation crosslinked medical grade ultrahigh molecular weight polyethylene. Journal of Biomedical Materials Research, 46(4), 573–581.

Baker, D. A., Hastings, R. S., Pruitt, L., 2000. Compression and tension fatigue resistance of medical grade ultra high molecular weight polyethylene: The effect of morphology, sterilization, aging and temperature. Polymer, 41(2), 795–808.

Baker, D.A., Bellare, A., Pruitt, L., 2003. The effects of degree of crosslinking on the fatigue crack initiation and propagation resistance of orthopedic-grade polyethylene. Journal of Biomedical Materials Research Part A An Official Journal of The Society for Biomaterials, The Japanese Society for Biomaterials, and The Australian Society for Biomaterials and the Korean Society for Biomaterials 66(1), 146–154.

Banasiak, D.H., Grandt, A.F., Montulli, L.T., 1977. Fatigue crack retardation in polycarbonate. Journal of Applied Polymer Science 21, 1297–1309.

Barsom, J., & Rolfe, S. (1999). Fatigue Crack Initiation. In Fracture and Fatigue Control In Structures: Applications of Fracture Mechanics (3rd ed., pp. 182–192). American Society for Testing and Materials.

Beardmore, P., Rabinowitz, S., 1975. Treatment Materials Science and Technology 6, 267.

Berrehili, A., Nadot, Y., Castagnet, S., Grandidier, J.C., Dumas, C., 2010. Multiaxial fatigue criterion for polypropylene – Automotive applications. International Journal of Fatigue 32, 1389–1392.

Bistolfi, A., Giustra, F., Bosco, F., Sabatini, L., Aprato, A., Bracco, P., & Bellare, A., 2021. Ultra-high molecular weight polyethylene (UHMWPE) for hip and knee arthroplasty: The present and the future. Journal of Orthopaedics, 25, 98–106. https://doi.org/10.1016/j.jor.2021.04.004

Bracco, P., Oral, E., 2011. Vitamin E-stabilized UHMWPE for Total Joint Implants: A Review. Clinical Orthopaedics and Related Research®, 469(8), 2286–2293.

Bradford, L., Baker, D., Ries, M. D., Pruitt, L. A., 2004. Fatigue Crack Propagation Resistance of Highly Crosslinked Polyethylene. Clinical Orthopaedics and Related Research, 429, 68.

Bucknall, C.B., Stevens, W.W., 1978. Toughening of Plastics. London: Plastics and Rubber Institute, pp. 24.

Charles, D.F., Gnanamoorthy, R., Ravindran, P., 2010. Rolling contact fatigue behavior of polyamide clay reinforced nanocomposite – Effect of load and speed. Wear 269, 565–571.

Charnley, J., 1961. ARTHROPLASTY OF THE HIP: A New Operation. The Lancet, 277(7187), 1129–1132.

Charnley, J. (1973). Arthroplasty of the Hip: A New Operation. Clinical Arthropaedics and Related Research, 95, 4–8.

Clark, T.R., Hertzberg, R.W., Nohammadi, N., 1991. In: Bg, A. (Ed.), Proceedings of 8th International Conference on Deformation, Yield and Fracture of Polymers. London: Plastics and Rubber Institute, pp. 31.

Cole, J. C., Lemons, J. E., & Eberhardt, A. W. (2002). Gamma irradiation alters fatigue-crack behavior and fracture toughness in 1900H and GUR 1050 UHMWPE. Journal of Biomedical Materials Research, 63(5), 559–566. https://doi.org/10.1002/jbm.10335

Connelly, G.M., Rimnac, C.M., Wright, T.M., Hertzberg, R.W., Manson, J.A., 1984. Fatigue crack propagation behavior of ultrahigh molecular weight polyethylene. Journal of Orthopaedic Research 2, 119–125.

Davidson, D., & Suresh, S. (1984). Fatigue Crack Growth Threshold Concepts. Proceedings of the International Symposium of Fatigue Crack Growth Threshold Concepts AIME.

Dawes, K., Glover, L.C., 1996. Effects of electron beam and irradiation on polymeric materials. In: Mark, J.E. (Ed.), Physical Properties of Polymers Handbook. New York, NY: AIP Press, pp. 557–576.

Dowling, N., 1993. Mechanical Behavior of Materials. Englewood Cliffs, New Jersey: Prentice Hall.

Eftekhari, M., Fatemi, A., 2016. On the strengthening effect of increasing cycling frequency on fatigue behavior of some polymers and their composites: Experiments and modeling. International Journal of Fatigue 87, 153–166.

Elber, W., 1970. Fatigue crack closure under cyclic tension. Engineering Fracture Mechanics 2, 37–45.

Estevez, R., Van der Giessen, E., 2005. Modeling and computational analysis of fracture of glassy polymers. In: Kausch, H.-H. (Ed.), Intrinsic Molecular Mobility and Toughness of Polymers II. Springer, pp.188.

Evans, A.G., Ahmad, Z.B., Gilbert, D.G., Beaumont, P.W.R., 1986. Mechanisms of toughening in rubber toughened polymers. Acta Metallurgica 34, 79–87.

Fan, Z., Yan, L., Liu, H., Li, X., Fan, K., Liu, Q., Li, J. J., Wang, B., 2023. The prevalence of hip osteoarthritis: A systematic review and meta-analysis. Arthritis Research & Therapy, 25(1), 51.

Ferry, J.D., 1961. Viscoelastic Properties of Polymers. New York: Wiley.

Furmanski, J., Pruitt, L. A., 2007. Peak stress intensity dictates fatigue crack propagation in UHMWPE. Polymer, 48(12), 3512–3519.

Furmanski, J., Anderson, M., Bal, S., Greenwald, A. S., Halley, D., Penenberg, B., Ries, M., Pruitt, L., 2009. Clinical fracture of cross-linked UHMWPE acetabular liners. Biomaterials, 30(29), 5572–5582.

Furmanski, J., Rimnac, C. M., & Pruitt, L. A., 2009. Brittle fatigue crack propagation in UHMWPE and its implications for total joint replacements. 14th International Conference on Deformation, Yield and Fracture of Polymers, Kerkrade, The Netherlands.

Furmanski, J., Kraay, M. J., Rimnac, C. M., 2011. Crack Initiation in Retrieved Cross-Linked Highly Cross-Linked Ultrahigh-Molecular-Weight Polyethylene Acetabular Liners: An Investigation of 9 Cases. The Journal of Arthroplasty, 26(5), 796–801.

Furmanski, J., & Rimnac, C. M., 2011. Crack Propagation Resistance Is Similar Under Static and Cyclic Loading in Crosslinked UHMWPE: A Pilot Study. Clinical Orthopaedics & Related Research, 469(8), 2302–2307. https://doi.org/10.1007/s11999-010-1712-y

Furmanski, J., Pruitt, L. A., 2018. Static mode fatigue crack propagation and generalized stress intensity correlation for fatigue–brittle polymers. International Journal of Fracture, 210(1), 213–221.

Garcea, S.C., Mavrogordato, M.N., Scott, A.E., Sinclair, I., Spearing, S.M., 2014. Fatigue micromechanism characterisation in carbon fibre reinforced polymers using synchrotron radiation computed tomography. Composites Science and Technology 99, 22–30.

Garcea, S.C., Sinclair, I., Spearing, S.M., 2015. In situ synchrotron tomographic evaluation of the effect of toughening strategies on fatigue micromechanisms in carbon fibre reinforced polymers. Composites Science and Technology 109, 32–39.

Gencur, S. J., Rimnac, C. M., Kurtz, S. M., 2003. Failure micromechanisms during uniaxial tensile fracture of conventional and highly crosslinked ultra-high molecular weight polyethylenes used in total joint replacements. Biomaterials, 24(22), 3947–3954.

Gencur, S.J., Rimnac, C.M., Kurtz, S.M., 2006. Fatigue crack propagation resistance of virgin and highly crosslinked, thermally treated ultra-high molecular weight polyethylene. Biomaterials 27(8), 1550–1557.

Goldman, M., Gronsky, R., Pruitt, L., 1998. The influence of sterilization technique and aging on the structure and morphology of medical-grade ultrahigh molecular weight polyethylene. Journal of Materials Science Materials in Medicine 9, 207–212.

Goldman, M., Pruitt, L., 1998. Comparison of the effects of gamma radiation and low temperature hydrogen peroxide gas plasma sterilization on the molecular structure, fatigue resistance, and wear behavior of UHMWPE. Journal of Biomedical Materials Research 40, 378–384.

Green, T., Fisher, J., Stone, M., Wroblewski, B., Ingham, E., 1998. Polyethylene particles of a ‘critical size’are necessary for the induction of cytokines by macrophages in vitro. Biomaterials 19(24), 2297–2302.

Green, T.R., Fisher, J., Matthews, J.B., Stone, M.H., Ingham, E., 2000. Effect of size and dose on bone resorption activity of macrophages by in vitro clinically relevant ultra high molecular weight polyethylene particles. Journal of Biomedical Materials Research 53(5), 490–497.

Harris, J.S., Ward, I.M., 1973. Fatigue-crack propagation in vinyle urethane polymers. Journal of Materials Science 8, 1655–1665.

Hertzberg, R., Nordberg, H., & Manson, J. (1970). Fatigue Crack Propagation in Polymeric Materials. Journal of Materials Science, 5(6), 521–526.

Hertzberg, R.W., Manson, J.A., Skibo, M., 1975. Frequency sensitivity of fatigue processes in polymeric solids. Polymer Engineering & Science 15, 252–260.

Hertzberg, R.W., Skibo, M.D., Manson, J.A., 1978. Fatigue Fracture Micromechanisms in Engineering Plastics Fatigue Mechanisms, ASTM STP 675. Philadelphia, PA: American Society for Testing and Materials, pp. 471–491.

Hertzberg, R.W., Manson, J.A., 1980. Fatigue of Engineering Plastics. New York, NY: Academic Press.

Hertzberg, R.W., Manson, J.A., 1983. Environment, frequency and temperature effects on fatigue in engineering plastics. In: Burke, J.J., Weiss, V. (Eds.), Sagamore Army Materials Research Conference Proceedings, vol. 27. Boston, MA: Springer.

Hertzberg, R.W., Manson, J.A., 1986. Encyclopedia of Polymer Science and Engineering. New York: Wiley, pp. 378.

Hertzberg, R.W., 1996. Deformation and Fracture Mechanics of Engineering Materials, fourth ed. New York, NY: Wiley.

Hertzberg, R., Vinci, R., & Hertzberg, J., 2012. Fatigue Crack Propagation. In Deformation and Fracture Mechanics of Engineering Materials (5th ed., pp. 569–644). John Wiley and Sons.

Hip & Knee Revision Surgery Recovery Timeline. (2021, April 6). University of Utah Health | University of Utah Health. https://healthcare.utah.edu/orthopaedics/specialties/joint-replacement/hip-knee-revision/recovery

Kanters, M.J.W., Stolkb, J., Govaerta, L.E., 2015. Direct comparison of the compliance method with optical tracking of fatigue crack propagation in polymers. Polymer Testing 46, 98–107.

Kinloch, A.J., Guild, F.J., 1996. Predictive modelling of the properties and toughness of rubber-toughened epoxies. In: Keith, C. (Ed.), Advances in Chemistry, Series 252: Toughened Plastics II: Novel Approaches in Science and Engineering. Washington, DC: American Chemical Society, pp. 1–25.

Kishi, H., Matsuda, S., Imade, J., et al., 2021. The effects of the toughening mechanism and the molecular weights between cross-links on the fatigue resistance of epoxy polymer blends. Polymer 223. 123712.

Klapperich, C., Komvopoulos, K., Pruitt, L., 1999. Tribological Properties and Microstructure Evolution of Ultra-High Molecular Weight Polyethylene. Journal of Tribology, 121(2), 394–402.

Kramer, E.J., Berger, L.L., 1990. Fundamental processes of craze growth and fracture. In: Kausch, H.H. (Ed.), Advances in Polymer Science, vol. 91/92. Berlin: Springer, pp. 1–68.

Krause, D., 2016. A physically based micromechanical approach to model damage initiation and evolution of fiber reinforced polymers under fatigue loading conditions. Composites Part B Engineering 87, 176–195.

Krzypow, David J., Rimnac, Clare M., 2000. Cyclic steady state stress–strain behavior of UHMW polyethylene. Biomaterials vol 21, 2081–2087.

Kurtz, S.M., Bartel, D.L., Rimnac, C.M., 1994. Transactions of the 40th Annual Meeting Of The Orthopedic Research Society. San Francisco: Orthopaedic Research Society.

Kurtz, S., et al., 2005. Prevalence of primary and revision total hip and knee arthroplasty in the United States from 1990 through 2002. The Journal of Bone and Joint Surgery 87(7), 1487–1497.

Kurtz, S., Ong, K., Lau, E., Mowat, F., Halpern, M., 2007. Projections of Primary and Revision Hip and Knee Arthroplasty in the United States from 2005 to 2030: The Journal of Bone & Joint Surgery, 89(4), 780–785.

Kurtz, S. M., 2009. UHMWPE Biomaterials Handbook: Ultra High Molecular Weight Polyethylene in Total Joint Replacement and Medical Devices. Academic Press.

Kurtz, S. M., Lau, E., Ong, K., Zhao, K., Kelly, M., Bozic, K. J., 2009. Future Young Patient Demand for Primary and Revision Joint Replacement: National Projections from 2010 to 2030. Clinical Orthopaedics and Related Research®, 467(10), 2606.

Kurtz, S. M., Oral, E., 2016. In Vivo Oxidation of UHMWPE. In S. M. Kurtz (Ed.), UHMWPE Biomaterials Handbook (Third Edition) (pp. 488–505). William Andrew Publishing.

Lampman, S., 2003. Characterization and Failure Analysis of Plastics. ASM International.

Landel, R.F., Nielsen, L.E., 1993. Mechanical Properties of Polymers and Composites. CRC press.

Lang, R.W., Manson, J.A., Hertzberg, R.W., Schirrer, R., 1984. Craze development in poly(methl methacrylate) during stable fatigue crack propagation. Polymer Engineering & Science 24, 833–842.

Loos, M.R., Yang, J., Feke, D.L., et al., 2013. Enhancement of fatigue life of polyurethane composites containing carbon nanotubes. Composite Part B 44, 740–744.

Malito, L. G., Arevalo, S., Kozak, A., Spiegelberg, S., Bellare, A., Pruitt, L., 2018. Material properties of ultra-high molecular weight polyethylene: Comparison of tension, compression, nanomechanics and microstructure across clinical formulations. Journal of the Mechanical Behavior of Biomedical Materials, 83, 9–19.

Malito, L. G., Sov, J. V., Gludovatz, B., Ritchie, R. O., & Pruitt, L. A., 2019. Fracture toughness of ultra-high molecular weight polyethylene: A basis for defining the crack-initiation toughness in polymers. Journal of the Mechanics and Physics of Solids, 122, 435–449. https://doi.org/10.1016/j.jmps.2018.09.022

Manson, J.A., Hertzberg, R.W., Bretz, P.E., 1981. Normalization of fatigue crack propagation behavior in polymers. In: Francois, D. (Ed.), Advances in Fracture Research. Oxford: Pergamon Press, pp. 443–448.

Mars, W.V., Fatemi, A., 2004. Factors that affect the fatigue life of rubber: A literature survey. Rubber Chemistry and Technology 77, 391–412.

Medel, F. J., Peña, P., Cegoñino, J., Gómez-Barrena, E., Puértolas, J. A., 2007. Comparative fatigue behavior and toughness of remelted and annealed highly crosslinked polyethylenes. Journal of Biomedical Materials Research Part B: Applied Biomaterials, 83B(2), 380–390.

Medel, F., Kurtz, S.M., Klein, G., et al., 2009. Revisiting the clinical wear performance of poly II tibial inserts after long-term implantation. In: Proceedings of the Transaction of the 2009 AAOS Meeting, Las Vegas.

Mills, N.J., Walker, N., 1976. Craze growth and crack growth in poly(viny chloride) under monotonic and fatigue loading. Polymer 17, 335–344.

Miner, M. A., 1945. Cumulative Damage in Fatigue. Journal of Applied Mechanics, 12(3), A159–A164.

Mortazavian, S., Fatemi, A., 2015. Fatigue behavior and modeling of short fiber reinforced polymer composites: A literature review. International Journal of Fatigue 70, 297–321.

Moskala, E.J., 1991. In: Proceedings of 8th International Conference on Deformation, Yield and Fracture of Polymers, Plastics and Rubber Institute, London 51/1.

Movahedi-Rad, A.V., Keller, T., Vassilopoulos, A.P., 2019. Modeling of fatigue behavior based on interaction between time-and cyclic-dependent mechanical properties. Composites Part A Applied Science and Manufacturing 124, 105469.

Mukherjee, B., Burns, D. J., 1971. Fatigue-crack growth in polymethylmethacrylate: Effect of frequency, mean and range of stress-intensity factor are covered by the authors in this paper. Experimental Mechanics, 11, 433-439.

Murakami, R., Noguchi, S., Akizono, K., Ferguson, W.G., 1987. Fatigue crack propagation and crack closure behavior in polycarbonate and fibre reinforced polycarbonate. Fatigue 10, 461–470.

Naebe, M., Abolhasani, M.M., Khayyam, H., Amini, A., Fox, B., 2016. Crack Damage in Polymers and Composites: A Review. Polymer Reviews 56(1), 31–69.

Nibur, K. A., & Somerday, B. P. (2025). Evaluating methods to reduce duration of near-threshold fatigue crack growth rate measurements for low-alloy steels in hydrogen gas. International Journal of Fatigue, 109150. https://doi.org/10.1016/j.ijfatigue.2025.109150

Niinomi, M., Wang, L., Enjitsu, T., & Fukunaga, K.-I. (2001). Fatigue characteristics of ultra high molecular weight polyethylene with different molecular weight for implant material. Journal of Materials Science: Materials in Medicine, 12(3), 267–272. https://doi.org/10.1023/A:1008923401615

Nugent, M., Young, S. W., Frampton, C. M., Hooper, G. J., 2021. The lifetime risk of revision following total hip arthroplasty. The Bone & Joint Journal, 103-B(3), 479–485.

O'Connell, P.A., McKenna, G.B., 2002. Yield and crazing in polymers. In: Matyjaszewski, K. (Ed.), Encyclopedia of Polymer Science and Technology. Wiley.

Oral, E., Malhi, A. S., & Muratoglu, O. K. (2006). Mechanisms of decrease in fatigue crack propagation resistance in irradiated and melted UHMWPE. Biomaterials, 27(6), 917–925. https://doi.org/10.1016/j.biomaterials.2005.06.025

Oral, E., Muratoglu, O. K., 2011. Vitamin E diffused, highly crosslinked UHMWPE: A review. International Orthopaedics, 35(2), 215–223.

Osteoarthritis (OA) | Arthritis | CDC. (2020, August 4). https://www.cdc.gov/arthritis/basics/osteoarthritis.htm

Paris, P.C., Gomez, M.P., Anderson, W.P., 1961. A rational analytic theory of fatigue. Trends in Engineering 13, 9–14.

Pastukhov, L.V., Kanters, M.J.W., Engels, T.A.P., Govaert, L.E., 2020. Physical background of the endurance limit in poly(ether ketone). Journal of Polymer Science 58(5), 716–736.

Patten, E. W., Cruz, C., Mehdizadeh, A., Assadian, S., Pruitt, L. A., 2011a. Fatigue Crack Propagation of Ultra-High Molecular Weight Polyethylene – Conformity of Compact Tension Specimen Geometry to ASTM E647. Society For Biomaterials, Abstract #041.

Patten, E. W., Carney, M. E., Johnson, P. M., Hong, T., Almaguer, A. J., Pruitt, L. A., 2011b. A Multi-Directional Tribo-System: Testing the Wear of UHMWPE Under Sliding, Rolling, and Rotation. 1177–1178.

Pearson, R., Pruitt, L., 1999. Fatigue crack propagation in polymer blends. In: Paul, D.R., Bucknall, C.B. (Eds.), Polymer Blends Formulation and Performance 27. New York: John Wiley and Sons, Inc, pp. 269–299.

Pippan, R., Hohenwarter, A., 2017. Fatigue crack closure: A review of the physical phenomena. Fatigue & Fracture of Engineering Materials & Structures 40(4), 471–495.

Pitoniak, F.J., Grandt, A.F., Montulli, L.T., Packman, P.F., 1974. Fatigue crack retardation and closure in polymethylmethacrylate. Journal of Engineering Fracture Mechanics 6, 663–670.

Plummer, C.J.G., Kausch, H.H., 1996. Deformation and entanglement in semicrystalline polymers. Journal of Macromolecular Science, Part B Physics 35(3–4), 637–657.

Pruitt, L., Herman, R., Suresh, S., 1992. Fatigue crack growth in polymers subjected to fully compressive cyclic loads. Journal of Materials Science 27, 1608–1616.

Pruitt, L., 1993. Cyclic Damage Ahead of Fatigue Cracks in Amorphous Solids: Theory, Experiments and Implications. In: Phd Thesis, Brown University.

Pruitt, L., Suresh, S., 1993. Cyclic stress-fields for fatigue cracks in amorphous solids experimental measurement and their implications. Philosophical Magazine A 67, 1219–1245.

Pruitt, L., Suresh, S., 1994. Cyclic stress-fields ahead of tension fatigue cracks in amorphous polymers. Polymer 35, 3221–3229.

Pruitt, L., Rondinone, D., 1996. The effect of specimen thickness and stress ratio on the fatigue behavior of polycarbonate. Polymer Engineering & Science 36, 1300–1305.

Pruitt, L., 2005. Deformation, yielding, fracture and fatigue behavior of conventional and highly cross-linked ultra high molecular weight polyethylene. Biomaterials, 905–915.

Pruitt, L. A., Simis, K. S., Bistolfi, A., Bellare, A., 2005. The Role of Microstructure on the Fatigue and Fracture Properties of Medical Grade Ultra High Molecular Weight Polyethylene. International Congress on Fracture ICF, 11.

Pruitt, L., & Furmanski, J. (2009). Polymeric biomaterials for load-bearing medical devices. JOM, 61(9), 14–20. https://doi.org/10.1007/s11837-009-0126-3

Pruitt, L.A., Chakravartula, A.M., 2011. Mechanics of Biomaterials: Fundamental Principles for Implant Design. Cambridge University Press.

Pruitt, L.A., Ansari, F., Kury, M., et al., 2013. Clinical trade-offs in cross-linked ultrahigh-molecular-weight polyethylene used in total joint arthroplasty. Journal of Biomedical Materials Research Part B Applied Biomaterials 101(3), 476–484.

Pruitt, L., Wat, A., Malito, L., 2022. Fatigue and Fracture Mechanisms in Polymers. In: Characterization and Failure Analysis of Plastics, ASM Handbook, 11B.

Pruitt, L., Roy, A., Smith, B., 2023. Fatigue of Polymers. In: Comprehensive Structural Integrity 2nd Edition 4, 146-161.

Quaresimin, M., Salviato, M., Zappalorto, M., 2015. Toughening mechanisms in nanoparticle polymer composites: experimental evidences and modeling. In Toughening Mechanisms in Composite Materials. Woodhead Publishing. pp. 113–133.

Ries, M. D., Pruitt, L., 2005. Effect of Cross-linking on the Microstructure and Mechanical Properties of Ultra-High Molecular Weight Polyethylene. Clinical Orthopaedics and Related Research (1976-2007), 440, 149–156.

Rimnac, C.M., Wright, T.M., Klein, R.W., 1988. J integral measurements of ultra high molecular weight polyethylene. Polymer Engineering & Science 28, 1586–1589.
Ritchie, R. O. (1977). Near-Threshold Fatigue Crack Propagation in Ultra-High Strength Steel: Influence of Load Ratio and Cyclic Strength. Journal of Engineering Materials and Technology, 99(3), 195–204. https://doi.org/10.1115/1.3443519

Ritchie, R.O., 1988. Mechanisms of fatigue crack propagation in metals, ceramics and composites: Role of crack tip shielding. Materials Science and Engineering 103, 15–28.

Ritchie, R.O., 2000. Mechanisms of fatigue crack propagation in ductile and brittle solids. International Journal of Fracture 100, 55–83.

Ritchie, R., 2002. Fatigue of brittle materials. In: Milne, I., Ritchie, R., Karihaloo, B.L. (Eds.), Comprehensive Structural Integrity Cyclic Loading and Fatigue. Elsevier.

Ritchie, R.O., Liu, D., 2021. Introduction to Fracture Mechanics. Elsevier. ISBN 978-0323898225.

Roy, A, 2024. Study of the Bio-Tribo-Mechanical Characteristics of Orthopedic-Grade Polymers. In: Ph.D. Thesis, UC Berkeley.

Sauer, J.A., Hara, M., 1990. Effect of molecular variable on crazing and fatigue. In: Kausch, H.H. (Ed.), Advances in Polymer Science, vol. 91/92. Berlin: Springer, pp. 69–118.

Sauer, J.A., Richardson, G.C., 1980. Fatigue of polymers. International Journal of Fracture 16, 499–532.

Saxena, A., Sudak, S., Donald, J., & Schmidt, D., 1978. Computer-Controlled Decreasing Stress Intensity Technique for Low Rate Fatigue Crack Growth Testing. Journal of Testing and Evaluation, 6(3).

Schmidt, R. A., & Paris, P. C., 1973. Threshold for Fatigue Crack Propagation and the Effects of Load Ratio and Frequency. Progress in Flaw Growth and Fracture Toughness Testing, ASTM STP 536, American Society for Testing & Materials, 79–94.

Scholz, R., Knyazeva, M., Porchetta, D., et al., 2018. Development of biomimetic in vitro fatigue assessment for UHMWPE implant materials. Journal of the Mechanical Behavior of Biomedical Materials 85, 94–101.

Sih, G.C., 1973. Handbook of Stress Intensity Factors. Bethlehem, PA: Lehigh University Press.

Simis, K. S., Bistolfi, A., Bellare, A., Pruitt, L. A., 2006. The combined effects of crosslinking and high crystallinity on the microstructural and mechanical properties of ultra high molecular weight polyethylene. Biomaterials, 27(9), 1688–1694.

Sirimamilla, P. A., Furmanski, J., Rimnac, C. M., 2011. Effect of Non-Uniform Material De-Cohesion on Crack Initiation From Notches in Crosslinked UHMWPE. ASME 2011 Summer Bioengineering Conference, Parts A and B, 1321–1322.

Sirimamilla, P. A., Furmanski, J., & Rimnac, C., 2013a. Peak stress intensity factor governs crack propagation velocity in crosslinked ultrahigh-molecular-weight polyethylene. Journal of Biomedical Materials Research Part B: Applied Biomaterials, 101B(3), 430–435. https://doi.org/10.1002/jbm.b.32850

Sirimamilla, P. A., Furmanski, J., Rimnac, C. M., 2013b. Application of viscoelastic fracture model and non-uniform crack initiation at clinically relevant notches in crosslinked UHMWPE. Journal of the Mechanical Behavior of Biomedical Materials, 17, 11–21.

Sirimamilla, P. A., Rimnac, C. M., Furmanski, J., 2018. Viscoplastic crack initiation and propagation in crosslinked UHMWPE from clinically relevant notches up to 0.5 mm radius. Journal of the Mechanical Behavior of Biomedical Materials, 77, 73–77.

Sirimamilla, A., Rimnac, C. M., 2019. Crack initiation from a clinically relevant notch in a highly-crosslinked UHMWPE subjected to static and cyclic loading. Journal of the Mechanical Behavior of Biomedical Materials, 91, 366–372.

Sobieraj, M. C., Kurtz, S. M., Rimnac, C. M., 2005. Notch strengthening and hardening behavior of conventional and highly crosslinked UHMWPE under applied tensile loading. Biomaterials, 26(17), 3411–3426.

Sobieraj, M. C., Kurtz, S. M., Wang, A., Manley, M. M., Rimnac, C. M., 2008. Notched stress–strain behavior of a conventional and a sequentially annealed highly crosslinked UHMWPE. Biomaterials, 29(35), 4575–4583.

Sobieraj, M. C., Rimnac, C. M., 2009. Ultra high molecular weight polyethylene: Mechanics, morphology, and clinical behavior. Journal of the Mechanical Behavior of Biomedical Materials, 2(5), 433–443.

Sobieraj, M. C., Murphy, J. E., Brinkman, J. G., Kurtz, S. M., Rimnac, C. M., 2013. Monotonic and fatigue behavior of five clinically relevant conventional and highly crosslinked UHMWPEs in the presence of stress concentrations. Journal of the Mechanical Behavior of Biomedical Materials, 28, 244–253.

Standard Test Method for Measurement of Fatigue Crack Growth Rates. (2024). https://store.astm.org/e0647-24.html

Suresh, S., 1983. Micromechanisms of fatigue crack growth retardation following overloads. Engineering Fracture Mechanics 18, 577–593.

Suresh, S., 1998. Fatigue of Materials, second ed. Cambridge: Cambridge University Press.

Takemori, M.T., 1982. Fatigue fracture of polycarbonate. Polymer Engineering & Science 22, 937–945.

Teoh, S.H., 2000. Fatigue of biomaterials: A review. International Journal of Fatigue 22(10), 825–837.

Total Hip Replacement—OrthoInfo—AAOS. (2024). https://www.orthoinfo.org/en/treatment/total-hip-replacement/

Total Knee Replacement—OrthoInfo—AAOS. (2024). https://www.orthoinfo.org/en/treatment/total-knee-replacement/

Williams, J. G., 1977. Fracture mechanics of polymers. Polymer Engineering & Science, 17(3), 144–149.

Wnuk, M.P., 1974. Quasi-static extension of a tensile crack contained in a viscoelastic-plastic solid. Journal of Applied Mechanics 41(1), 234–242.

Wright, T.M., Astion, D.J., Bansal, M., et al., 1988. Failure of carbon fiber-reinforced polyethylene total knee-replacement components. Journal of Bone and Joint Surgery 70(6), 926–932.

Wright, T.M., Rimnac, C.M., Stulberg, S.D., et al., 1992. Wear of polyethylene in total joint replacements – Observations from retrieved PCA knee implants. Clinical Orthopaedics 276, 126–134.

Yang, J., Liu, J., 2001. Cavitation of rubber particles in high-impact polystyrene. Polymer Journal 33(12), 952–954.

Zenkert, D., Burman, M., 2009. Tension, compression and shear fatigue of a closed cell polymer foam. Composites Science and Technology 69, 785–792.

Zhang, Y., Jordan, J. M., 2010. Epidemiology of Osteoarthritis. Clinics in Geriatric Medicine, 26(3), 355–369.

Zheng, X., et al., 2019. "Mechanical characteristics of medical grade UHMWPE under dynamic compression.". Journal of Materials Science Materials in Medicine 30.5, 1–12.

Zhou, J., Chakravartula, A., Pruitt, L., Komvopoulos, K., 2004. Tribological and Nanomechanical Properties of Unmodified and Crosslinked Ultra-High Molecular Weight Polyethylene for Total Joint Replacements. Journal of Tribology, 126(2), 386–394.

Zhou, J., Komvopoulos, K., 2005. Wear Mechanisms of Untreated and Gamma Irradiated Ultra-High Molecular Weight Polyethylene for Total Joint Replacements. Journal of Tribology, 127(2), 273–279.

Zhou, Y.Q., Brown, N., 1992. The mechanism of fatigue failure in a polyethylene copolymer. Journal of Polymer Science: Polymer Physics 30, 477–487.

Zysk, S., et al., 2005. Particles of all sizes provoke inflammatory responses in vivo. Clinical Orthopaedics and Related Research 433, 258–264.